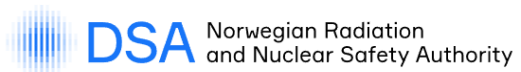


AMS, DSA AND NGU JOINT SURVEY REPORT OF NEVADA NATIONAL SECURITY SITE IN 2018



AERIAL CAMPAIGN US DOE AMS SURVEY RESULTS Nevada National Security Site April 16–20, 2018

US Department of Energy
National Nuclear Security Administration
Remote Sensing Laboratory
Aerial Measuring System (AMS)
Norwegian Radiation and Nuclear Safety Authority
(Direktoratet for strålevern og atomsikkerhet) (DSA)
Geological Survey of Norway (NGU)



This report was prepared as an account of work sponsored by an agency of the U.S. Government. Neither the U.S. Government nor any agency thereof, nor any of their employees, nor any of their contractors, subcontractors or their employees, makes any warranty or representation, express or implied, or assumes any legal liability or responsibility for the accuracy, completeness, or usefulness of any information, apparatus, product, or process disclosed, or represents that its use would not infringe privately own rights. Reference herein to any specific commercial product, process, or service by trade name, trademark, manufacturer, or otherwise, does not necessarily constitute or imply its endorsement, recommendation, or favoring by the U.S. Government or any agency thereof. The views and opinions of authors expressed herein do not necessarily state or reflect those of the U.S. Government or any agency thereof.

ABSTRACT

In April 2018, the U.S. Department of Energy (DOE), National Nuclear Security Administration (NNSA) Aerial Measuring System (AMS) and the Norwegian Radiation and Nuclear Safety Authority (DSA), conducted a series of joint surveys at various locations in Southern Nevada including the Nevada National Security Site (NNSS). The goal of this project was to compare the responses of the two agencies' aerial radiation detection systems and data analysis techniques. This test included varied radioactive surface contamination levels and isotopic composition experienced at the NNSS and the differing data processing techniques utilized by the respective teams. This joint survey follows the template of similar recent exchanges with Natural Resources Canada and French Institut de Radioprotection et de Sûreté Nucléaire.

During the joint survey AMS used a commercial gamma radiation detection system manufactured by Radiation Solutions Inc. (RSI), consisting of twelve 2"x4"x16" NaI (TI) (12 x 2 liter) scintillator crystals mounted in external pods with six crystals on each side of the DOE Bell 412 helicopter. The DSA team also used an RSI made detection system consisting of four 4" x 4" x 16" NaI(Tl) (4 x 4 liter) scintillator crystals mounted inside (behind the pilot seat) to the AMS aircraft. The DSA system ran in parallel to the AMS system to collect coincident data. The joint survey provided DSA an opportunity to characterize their system's response to various fission and activation product sources at the NNSS. Because AMS and DSA are both the national asset for airborne radiological emergency response in their respective countries', it is important for both assets to understand and characterize their relative detection system response in order to facilitate cooperation in a joint response to a radiological disaster. Geological Survey of Norway (NGU) was a part of the DSA team for data acquisition and processing. The results presented herein are for both the DOE/AMS and DSA portion of the flights and are accompanied with discussion of AMS and NGU data analysis techniques.

TABLE OF CONTENTS

ABSTRACT.....	2
TABLE OF CONTENTS.....	3
LIST OF FIGURES.....	5
INTRODUCTION	1
AERIAL RADIOMETRIC SURVEYING	2
Aerial Measuring System	2
DSA	8
NGU	10
DATA EVALUATION METHODS	10
AMS	10
DSA/NGU	14
DATA PREPARATION	15
Gross count and man-made gross count	15
Individual nuclides identification	15
Gridding/contouring and color scales	15
ORGANIZATION OF THE CAMPAIGN	16
Joint Survey Activity Plan.....	16
Description of Survey Sites	16
AMS AND NGU RESULTS.....	20
Attenuation and Sensitivity	20

Spectral Extractions	24
DATA PRODUCTS	27
Product Presentation	27
Natural Background at Government Wash.....	28
NNSS Area 3.....	30
NNSS Area 8.....	32
NNSS Area 11.....	34
NNSS Area 30.....	36
CONCLUSION	38
BIBLIOGRAPHY.....	39
APPENDIX A: PERSONNEL.....	40
APPENDIX B: ADDITIONAL EXTRACTIONS	41
Government Wash.....	43
Area 3	46
Area 8	50
Area 11	54
Area 30	56

LIST OF FIGURES

FIGURE 1. DOE BELL 412 HELICOPTER AT DESERT ROCK AIRPORT.	2
FIGURE 2. AMS RSI SYSTEM COMPONENTS.	3
FIGURE 3. RSX-3 BOX WITH THREE 2" X 4" X 16" NAI(TL) CRYSTALS.	4
FIGURE 4. THE RS-701 CONSOLE ON TOP OF THE RSX-3 DETECTOR BOX.	4
FIGURE 5. RS-501 AGGREGATOR CONSOLE WITH THE TRIMBLE GPS RECEIVER.....	5
FIGURE 6. AVID 3.8 LAUNCHER SCREEN.	6
FIGURE 7. AVID USER SCREEN IN A TYPICAL FLIGHT CONFIGURATION.	7
FIGURE 8. TRIMBLE STEERING SYSTEM IN USE DURING AMS FLIGHT.	7
FIGURE 9. INSTALLATION OF THE DSA SYSTEM ON THE DOE BELL 412 HELICOPTER.....	8
FIGURE 10. INTERALLY MOUNTED RSI DETECTOR AND SUPPORT SYSTEM. ON THE LEFT ARE THE TWO RSX-1 CRYSTALS AND RSN-4 NEUTRON DETECTOR, AND ON THE RIGHT IS THE CONTROLLING LAPTOP. EQUIPMENT WAS STRAPPED TO TIE DOWNS IN THE AIRCRAFT.	9
FIGURE 11. RADASSIST DATA ACQUISITION SCREEN AVAILABLE TO USER FOR QUALITY CONTROL.	10
FIGURE 12. EXAMPLE OF THE GAUSSIAN FIT TO CS-137 PEAK IN AVID.....	14
FIGURE 13. PROPOSED SURVEY SETUP AT THE GOVERNMENT WASH SITE.	16
FIGURE 14. THE LAND AND WATER CALIBRATION LINES AT THE LAKE MOHAVE CALIBRATION RANGE.	17
FIGURE 15. LOCATIONS OF COMMON SURVEY AREAS AT THE NNSS.....	19
FIGURE 16. GROSS GAMMA COUNT RATE TIME SERIES OVER THE LAND CALIBRATION LINE FOR THE AMS SYSTEM.	20
FIGURE 17. GROSS GAMMA COUNT RATE TIME SERIES OVER THE WATER LINE FOR THE AMS SYSTEM.....	21
FIGURE 18. GROSS GAMMA COUNT RATE TIME SERIES OVER THE LAND LINE FOR THE DSA SYSTEM PLOTTED BY NGU.....	21
FIGURE 19. GROSS GAMMA COUNT RATE TIME SERIES OVER THE WATER LINE FOR THE DSA SYSTEM PLOTTED BY NGU.....	21
FIGURE 20. LOG PLOT OF NET GAMMA COUNTS VS ALTITUDE USED TO CALCULATE HEIGHT ATTENUATION.	23
FIGURE 21. LOG PLOT OF AVERAGE NET GAMMA COUNTS VS ALTITUDE USED TO CALCULATE HEIGHT ATTENUATION BY NGU.	23
FIGURE 22. COMPTON BACKGROUND CORRECTION.	26
FIGURE 23. GROSS COUNT OF THE NATURAL BACKGROUND AREA (GOVERNMENT WASH) FROM AMS DATA.	28
FIGURE 24. GROSS COUNTS OF THE NATURAL BACKGROUND AREA (GOVERNMENT WASH) FROM DSA DATA.	28
FIGURE 25. DOSE RATE OF THE NATURAL BACKGROUND AREA (GOVERNMENT WASH) FROM AMS DATA.	29
FIGURE 26. DOSE RATE OF THE NATURAL BACKGROUND AREA (GOVERNMENT WASH) FROM DSA DATA.	29
FIGURE 27. GROSS COUNTS FROM NNSS AREA 3 FROM AMS DATA.	30
FIGURE 28. GROSS COUNTS FROM NNSS AREA 3 FROM DSA DATA.	30
FIGURE 29. DOSE RATE FROM NNSS AREA 3 FROM AMS DATA.....	31
FIGURE 30. DOSE RATE FROM NNSS AREA 3 FROM DSA DATA.....	31
FIGURE 31. GROSS COUNTS FROM NNSS AREA 8 FROM AMS DATA.	32
FIGURE 32. GROSS COUNTS FROM NNSS AREA 8 FROM DSA DATA.	32
FIGURE 33. DOSE RATE FROM NNSS AREA 8 FROM AMS DATA.....	33

FIGURE 34. DOSE RATE FROM NNSS AREA 8 FROM DSA DATA.....	33
FIGURE 35. GROSS COUNTS FROM NNSS AREA 11 FROM AMS DATA.	34
FIGURE 36. GROSS COUNTS FROM NNSS AREA 11 FROM DSA DATA.	34
FIGURE 37. DOSE RATE FROM NNSS AREA 11.	35
FIGURE 38. DOSE RATE FROM NNSS AREA 11 FROM DSA DATA.....	35
FIGURE 39. GROSS COUNTS FROM NNSS AREA 30 FROM AMS DATA.	36
FIGURE 40. GROSS COUNTS FROM NNSS AREA 30 FROM DSA DATA.	36
FIGURE 41. DOSE RATE FROM NNSS AREA 30 FROM AMS DATA.....	37
FIGURE 42. DOSE RATE FROM NNSS AREA 30 FROM DSA DATA.....	37
FIGURE 43. POTASSIUM (%) FROM THE NATURAL BACKGROUND AREA (GOVERNMENT WASH) FROM AMS DATA.	43
FIGURE 44. POTASSIUM (CPS) FROM THE NATURAL BACKGROUND AREA (GOVERNMENT WASH) FROM DSA DATA.	43
FIGURE 45. URANIUM (PPM) FROM THE NATURAL BACKGROUND AREA (GOVERNMENT WASH) FROM AMS DATA.	44
FIGURE 46. URANIUM (CPS) FROM THE NATURAL BACKGROUND AREA (GOVERNMENT WASH) FROM DSA DATA.	44
FIGURE 47. THORIUM (PPM) FROM THE NATURAL BACKGROUND AREA (GOVERNMENT WASH) FROM AMS DATA.	45
FIGURE 48. THORIUM (CPS) FROM THE NATURAL BACKGROUND AREA (GOVERNMENT WASH) FROM DSA DATA.	45
FIGURE 49. MMGC (C_{MM}) FROM NNSS AREA 3 FROM DSA DATA	46
FIGURE 50. CS-137 EXTRACTION (GAUSSIAN) FROM NNSS AREA 3 FROM AMS DATA.	47
FIGURE 51. CS-137 EXTRACTION (SPECTRAL WINDOW) FROM NNSS AREA 3 FROM DSA DATA.	47
FIGURE 52. EU-152 EXTRACTION (TWO-WINDOW) FROM NNSS AREA 3 FROM AMS DATA.	48
FIGURE 53. EU-152 EXTRACTION (SPECTRAL WINDOW) FROM NNSS AREA 3 FROM DSA DATA.	48
FIGURE 54. AM-241 EXTRACTION (TWO-WINDOW) FROM NNSS AREA 3 FROM AMS DATA.	49
FIGURE 55. AM-241 EXTRACTION (SPECTRAL WINDOW) FROM NNSS AREA 3 FROM DSA DATA.....	49
FIGURE 56. MMGC (C_{MM}) FROM NNSS AREA 8 FROM DSA DATA.	50
FIGURE 57. CS-137 EXTRACTION (TWO-WINDOW) FROM NNSS AREA 8 FROM AMS DATA.....	51
FIGURE 58. CS-137 EXTRACTION (SPECTRAL WINDOW) FROM NNSS AREA 8 FROM DSA DATA.	51
FIGURE 59. CO-60 EXTRACTION (TWO-WINDOW) FROM NNSS AREA 8 FROM AMS DATA.	52
FIGURE 60. AM-241 EXTRACTION (TWO-WINDOW) FROM NNSS AREA 8 FROM AMS DATA.	53
FIGURE 61. AM-241 EXTRACTION (SPECTRAL WINDOW) FROM NNSS AREA 8 FROM DSA DATA.....	53
FIGURE 62. MMGC (C_{MM}) FROM NNSS AREA 11 FROM DSA DATA.	54
FIGURE 63. AM-241 EXTRACTION (TWO-WINDOW) FROM NNSS AREA 11 FROM AMS DATA.	55
FIGURE 64. AM-241 EXTRACTION (SPECTRAL WINDOW) FROM NNSS AREA 11 FROM DSA DATA.....	55
FIGURE 65. MMGC (C_{MM}) FROM NNSS AREA 30 FROM DSA DATA.	56
FIGURE 66. CS-137 EXTRACTION (TWO-WINDOW) FROM NNSS AREA 30 FROM AMS DATA.....	57
FIGURE 67. Cs-137 EXTRACTION (SPECTRAL WINDOW) FROM NNSS AREA 30 FROM DSA DATA.....	57
FIGURE 68. EU-152 EXTRACTION (TWO-WINDOW) FROM NNSS AREA 30 FROM AMS DATA.	58
FIGURE 69. AM-241 EXTRACTION (TWO-WINDOW) FROM NNSS AREA 30 FROM AMS DATA.	59
FIGURE 70. AM-241 EXTRACTION (SPECTRAL WINDOW) FROM NNSS AREA 30 FROM DSA DATA.....	59

List of Tables

TABLE 1. AVERAGE GROSS COUNT RATES FROM AMS DETECTOR SYSTEM AT THE CALIBRATION LINE.	22
TABLE 2. AVERAGE GROSS COUNT RATES CALCULATED BY NGU FROM DSA DETECTOR SYSTEM AT THE CALIBRATION LINE.	22
TABLE 3. HEIGHT ATTENUATION AND COUNT TO EXPOSURE RATE COEFFICIENTS (DSA DATA CALCULATED BY AMS).	24
TABLE 4. EXTRACTION WINDOWS AND METHODS.	24
TABLE 5. K VALUES DETERMINED FOR VARIOUS ISOTOPES FOR EACH AREA.	25
TABLE 6. EXTRACTION WINDOWS FOR NGU.	26
TABLE A1. DOE PERSONNEL.	40
TABLE A2. DSA/NGU PERSONNEL.	40
TABLE B1. MAXIMUM COUNTS/SECOND/CHANNEL FOR VARIOUS RADIO-ELEMENTS FROM VARIOUS NNSS TEST AREAS.	41
TABLE B2. ANTHROPOGENIC RADIO-NUCLIDES FOUND FROM AMS DATA BY AMS EXTRACTION METHOD AND FROM DSA DATA BY NGU EXTRACTION METHOD FROM VARIOUS NNSS TEST AREAS.	42

INTRODUCTION

The U.S. Department of Energy (DOE) Aerial Measuring System (AMS) and Norwegian Radiation and Nuclear Safety Authority (DSA) collaboration was inspired by previous exchanges that AMS has had with both the Canadian and French governments. AMS, based out of the Remote Sensing Laboratories (RSL), is a National Nuclear Security Administration (NNSA) nuclear and radiological emergency response asset. DSA is the radiation protection and nuclear safety organization for the Norwegian government. The Geological Survey of Norway (NGU) was a part of the DSA team for data acquisition and interpretation.

The intention of the joint survey was to conduct flights over the Nevada National Security Site (NNSS) to measure real anthropogenic ground contamination and compare processes and procedures of each country's aerial measuring system. These aerial measuring systems can detect and map ground contamination that may result from a nuclear/radiological accident/incident. The planning for the joint survey took place during November of 2017 and was executed the week of April 16, 2018.

Both AMS and DSA use a commercial Radiation Solutions Inc. (RSI) detection system. DSA's system was shipped to the RSL at Nellis Air Force Base in the days leading up to the survey and was installed on the AMS aircraft by AMS and DSA personnel.

AMS and DSA/NGU personnel each operated their own equipment during the survey. The arrangement of equipment and aircraft approximated configurations that are the standard for emergency response in each of the respective countries.

For both teams, the objectives of this joint survey were to:

- Gain equipment familiarization across emergency response organizations
- Compare technologies, procedures, and data analysis techniques
- Examine differences in system calibration and other techniques
- Exchange ideas related to best practices and future improvements

The DSA had one additional objective:

- DSA does not have access to a dedicated aircraft, the exchange provided an opportunity to exercise the portability of their system and its field installation on a chartered helicopter, especially in an international deployment with logistical challenges.

This report presents the measurements, data analysis, and results from both countries' assets.

AERIAL RADIOMETRIC SURVEYING

The primary advantage of acquiring aerial radiometric measurements over traditional ground-based techniques lies in the high collection rate of data over large areas and rough terrain. This measurement technique is used all over the world by many different scientific and governmental organizations. The goal of the survey is to achieve complete area coverage with overlapping footprint. This is accomplished by collecting measurements in a regular grid pattern generated from parallel flight lines. Flight altitude is kept constant during the measurement flight with typical values recorded between 50 ft (15 m) and 600 ft (182 m) above ground level (AGL). Gamma-ray spectra are recorded in regular time intervals of one second, yielding spatial integration over about 100 ft (30 m) of the flight line depending on altitude at a nominal velocity of 70 knots (130 km/hr), although actual speeds may vary due to many factors including rough terrain. Acquiring spectral data of this type allows separation of natural radioactivity from that of anthropogenic sources and identification of specific isotopes, whether natural or anthropogenic.

AERIAL MEASURING SYSTEM

The AMS acquisition platform consists of a series of DOE owned and mission dedicated airframes. In this survey series, the AMS Nellis Bell 412 helicopter (Figure 1) was equipped with a detection system developed by Radiation Solutions Incorporated (RSI) (Figure 2). RSI is a Canadian corporation specializing in manufacturing aerial radiation detection systems that are intended for geophysical research. The AMS detection system on the Bell 412 helicopter uses radar altimeter vertical positioning (average distance to the ground), and Differential Global Positioning Systems for 3D positioning.



FIGURE 1. DOE BELL 412 HELICOPTER AT DESERT ROCK AIRPORT.

The detection system employs a total of 12 thallium-doped sodium iodide NaI(Tl) crystals, as log-type detectors with dimensions of 2" × 4" × 16" (2 liters). These detectors are packaged in four RSX-3 units containing three crystals each. An RS-501 aggregator combines the inputs of each RSX-3/RS-701 unit. The unit also provides power distribution and differential GPS which is used to coordinate timing for data acquisition. The four RSX-3 boxes are fitted into the externally-mounted aluminum pods (two RSX-3 per pod) on both the left and right sides of the Bell 412 helicopter.



FIGURE 2. AMS RSI SYSTEM COMPONENTS.

Each 2" × 4" × 16" NaI(Tl) crystal is coupled to a photomultiplier tube that produces analog signals for digital analysis by the Advanced Digital Spectrometer (ADS) module. Each individual NaI(Tl) crystal detector has its own high-speed (60 MHz) analog-to-digital converter and a Digital Signal Processor (DSP)/field-programmable gate array assembly (Figure 3). This module converts the analog signal from the detector to a digital spectrum with a 10⁶ channel resolution.

Using a unique detector energy calibration curve stored in the ADS module, the spectrum is linearized and compressed to the system's native 1024 channels. The high-speed adaptive DSP processing allows each pulse to be corrected, if necessary, without distortion at very high data-throughput rates, up to 250,000 counts per second (cps)/crystal detector, and up to 10 Hz data sampling.

The resulting combination of minimal dead time, improved pulse pileup rejection, individual crystal linearization, and accurate detector summation produces exceptionally clean spectra. These spectra are fed by 1 Mbps RS-485 data connections to the RS-701 console. The detector processing unit continuously monitors the state of health of the individual crystals and the system. Each crystal is individually gain-stabilized using a multi-peak approach, effectively eliminating the

need for any pre-stabilization with external sources. This makes the unit ideal to handle the wide dynamic range of radiation data seen in airborne applications.



FIGURE 3. RSX-3 BOX WITH THREE 2" X 4" X 16" NAI(TL) CRYSTALS.

INTEGRATED CONSOLE (RS-701 CONSOLE)

Each of the four RSX-3 units is controlled by the RS-701 console mounted on top of the RSX-3 box (Figure 4). The console uses RSI proprietary analysis techniques to automatically adjust the gain of the detectors to compensate for changing temperature and aging drift effects. The system uses spectra of natural radioactive isotopes of uranium (U), potassium (K), and thorium (Th) present in all ground material to stabilize the system at startup and maintain this gain automatically during system use with no user input required. The RS-701 console has a built-in GPS receiver. However, as the AMS RSI system integrates multiple RS-701 consoles into the RS-501 aggregator, the built-in GPS receivers were used only as synchronizing timers and not for positioning.



FIGURE 4. THE RS-701 CONSOLE ON TOP OF THE RSX-3 DETECTOR BOX.

INTEGRATED CONSOLE (RS-501 AGGREGATOR)

The four RS-701 consoles are integrated into a single RS-501 aggregator, shown in Figure 5. The RS-501 aggregator combines the inputs of each RSX-3/RS-701 unit together and provides a power distribution unit and differential GPS. The RS-501 unit retains 96 15-minute files representing the last 24 hours of data acquisition recorded to a solid-state disk in a 24-hour circular buffer. The RS-501 is then finally interfaced with the laptop PC running the Advanced Visualization and Integration of Data (AVID) software used for system monitoring and real-time data display in flight.



FIGURE 5. RS-501 AGGREGATOR CONSOLE WITH THE TRIMBLE GPS RECEIVER.

AVID SOFTWARE

The AVID framework and associated modules (Figure 6) were developed, as a joint effort between the Remote Sensing Laboratory (RSL) and the Pacific Northwest National Laboratory (PNNL), for real-time acquisition, visualization, and analysis of radiation data from aerial and mobile detection systems. The AVID software is designed to support both data acquisition and analysis functionality for radiation detection systems. It is extensible and flexible in order to provide for the integration of various modules. Initial releases were developed upon the requirements defined in the AMS Software Modernization Requirements Document in 2010.

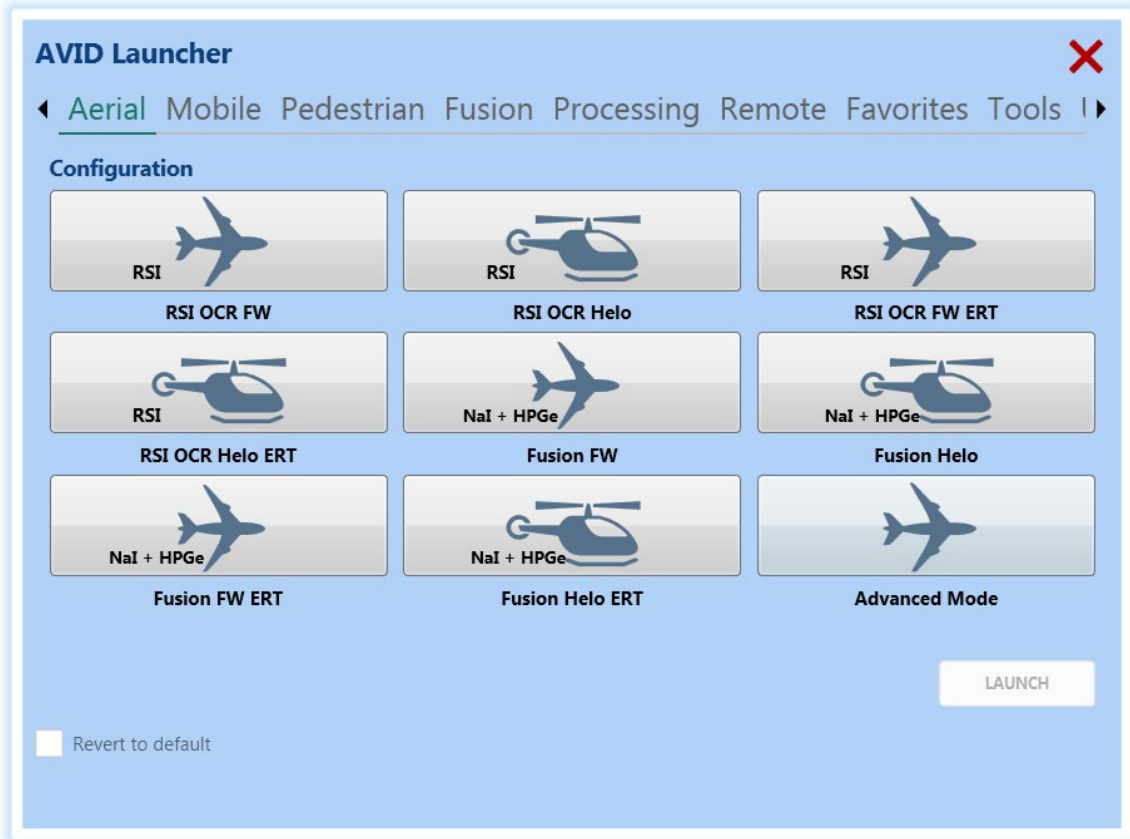


FIGURE 6. AVID 3.8 LAUNCHER SCREEN.

The AVID user screen presented in Figure 7 shows the typical, user-configurable screen layout for the aerial mission. However, this view can be quickly changed according to the mission's needs and the operator's personal preference. A similar arrangement of windows and tools are available in AVID's data processing modes.

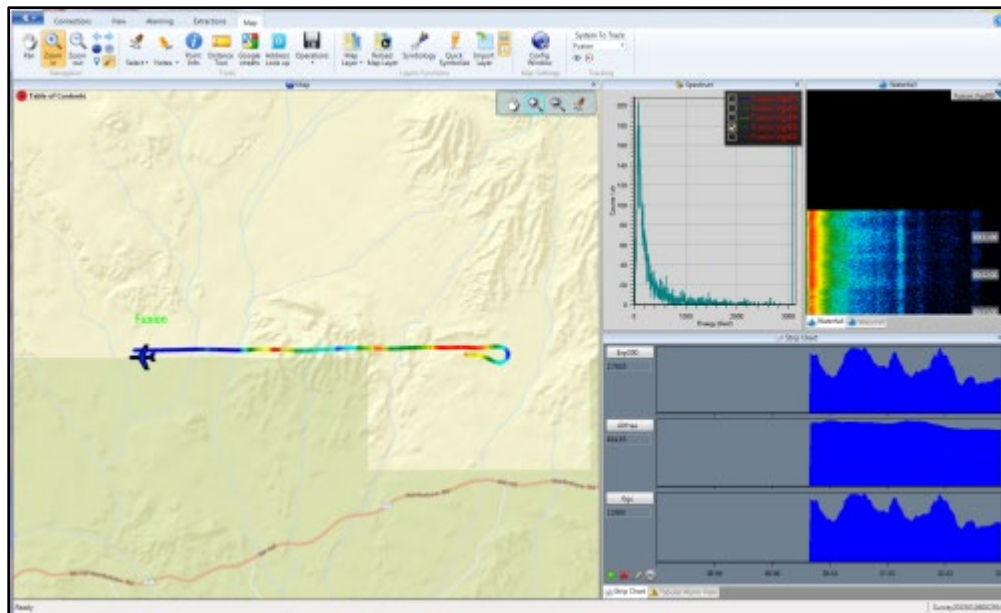


FIGURE 7. AVID USER SCREEN IN A TYPICAL FLIGHT CONFIGURATION.

NAVIGATION

For steering guidance provided to the pilots, AMS uses a commercial system from Trimble shown schematically and during flight in Figure 8. The system requires input of the flight area boundary and an “AB line” indicating flight direction. During flight, pilots are guided with the help of the light bar.

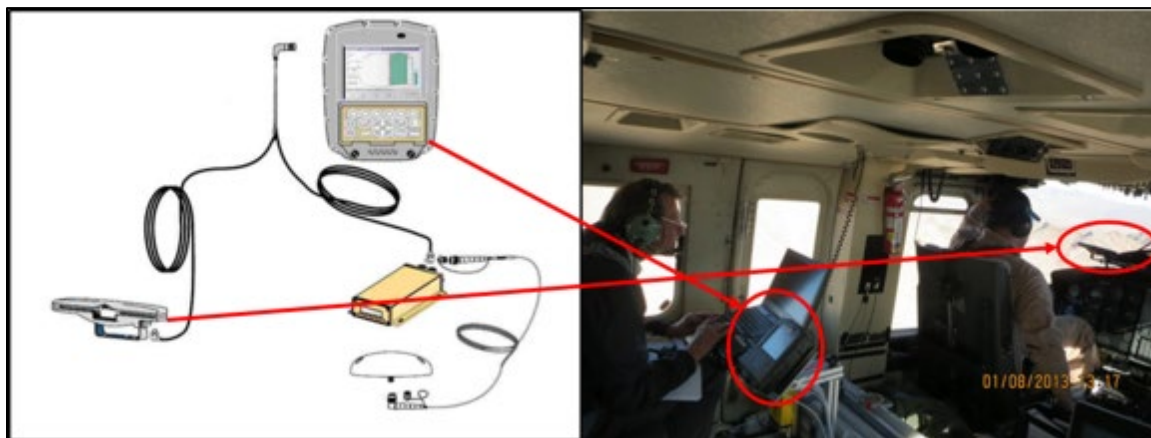


FIGURE 8. TRIMBLE STEERING SYSTEM IN USE DURING AMS FLIGHT.

DSA

DSAs response mission requires the ability to respond quickly to cover any location across a large geographical area. Depending on specific mission requirements and types of aircraft available, several detection system configurations, all based on RSI spectrometers, can be fielded. The DSA system (RS-500) is mounted on two 330 helicopters (Sea King) from The Norwegian Air Forces 330 and the Norwegian Coastal Administration's aircraft (LN-KYV RADIAC).

For the joint survey, DSA used a standard RSI Mobile Radiation Monitoring System RSX-4 with four 4" x 4" x 16" (10 cm x 10 cm x 40 cm), 16 liters of downward looking detector. The RSX-4 is a self-contained gamma-ray system. It can be used in land vehicles, helicopters, UAVs, or at a fixed location. The RSX-4 airborne spectrometer is supplied with the RadAssist application, a user monitoring and control software.

The RSX-4 system and associated electronics are mounted inside the DOE Bell 412 helicopter shown in Figures 9 & 10. The system comes with an inbuilt GPS receiver.



FIGURE 9. INSTALLATION OF THE DSA SYSTEM ON THE DOE BELL 412 HELICOPTER.



FIGURE 10. INTERNALLY MOUNTED RSI DETECTOR AND SUPPORT SYSTEM. ON THE LEFT ARE THE TWO RSX-1 CRYSTALS AND RSN-4 NEUTRON DETECTOR, AND ON THE RIGHT IS THE CONTROLLING LAPTOP. EQUIPMENT WAS STRAPPED TO TIE DOWNS IN THE AIRCRAFT.

DSA used a laptop PC running the RSI RadAssist software for data acquisition and detector performance monitoring in flight. The spectrometer was mounted behind the pilot seat inside the helicopter. A view of the RadAssist software is presented in Figure 11. RadAssist data acquisition screen is available for quality control. The operator can view the current spectrum, as well as a waterfall plot of the previous few minutes of acquisition. In addition, it is possible to configure the software to calculate in real-time various quantities from the data, such as counts with a given energy region of interest. Such quantities, in addition to being recorded with the data, can be viewed in strip chart format.

Data are recorded both internally in the console, on the laptop in RSI proprietary RSV format, and potentially in N42 format as well. Data are retained in the console for approximately twenty-four hours from the time of acquisition. DSA finds that extracting the data from the console, though slightly more work, provides the most complete and flexible data format for further processing.

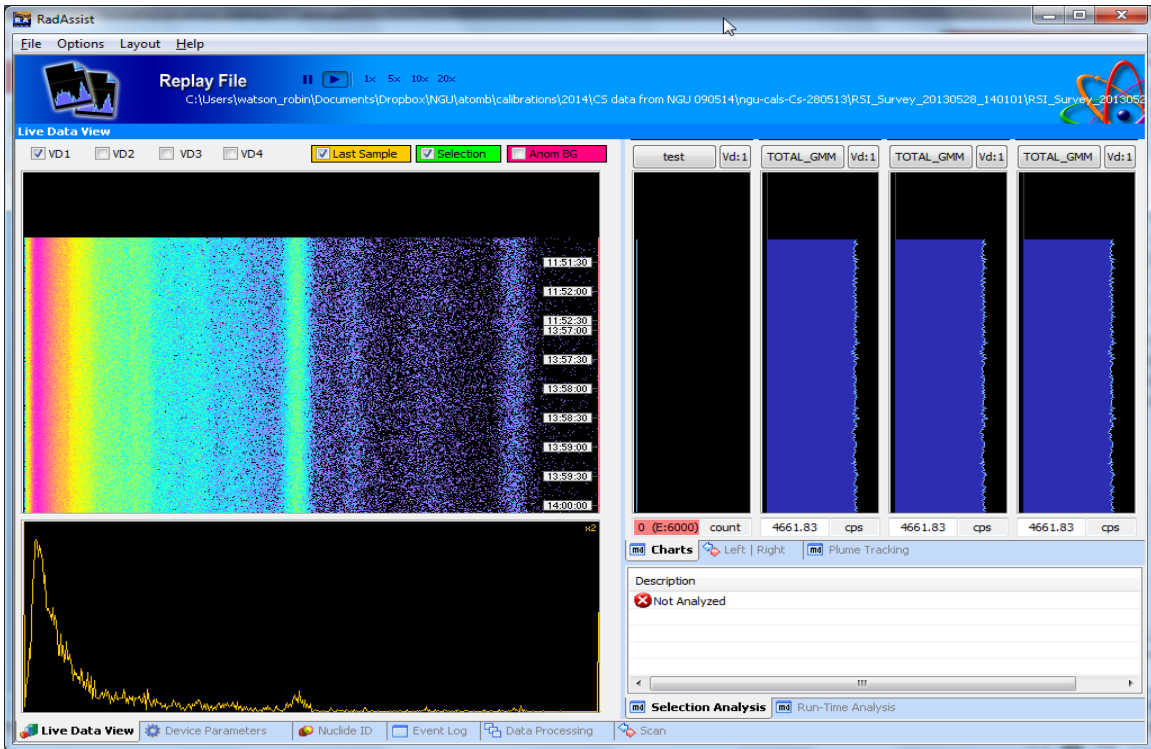


FIGURE 11. RADASSIST DATA ACQUISITION SCREEN AVAILABLE TO USER FOR QUALITY CONTROL.

NGU

NGU has an RSX-5 gamma-ray spectrometer consisting of 16 L downward looking and 4 L upward looking NaI (TI) detector. NGU rents helicopters to perform general geological surveys. NGU also mounts its RSX-5 spectrometer in a van to perform ground surveys and to participate in emergency nuclear accident preparedness programs. NGU uses RadAssist from RSI for data acquisition and in-house software for navigation. Gamma-ray spectrometry data are processed in Oasis montaj from Geosoft with in-house routines of NGU.

DATA EVALUATION METHODS

AMS

AMS uses its own data processing methodology, developed by AMS scientists and incorporated into the AVID framework. The collected spectral data are processed in several steps, starting with the correction of the gross counts to the nominal flight altitude, and for all background components (radon, cosmic, helicopter). These results can be used later for deriving terrestrial exposure rate, extracting anthropogenic activity, and finally extracting individual isotopes. All data are then presented as contour maps using the AVID software.

The RSI system records the latitude and longitude at the start of an acquisition period (1s). As the aircraft is moving at approximately 36 m/s, the actual measurement represents an integral over that time and distance rather than the measurement at a single point. It is therefore more spatially accurate to shift the latitude and longitude one-half of an acquisition period when interpolating over the dataset, this is referred to as 'time shift'. Without this time shift correction, a 'herringbone' effect is introduced into the dataset.

GROSS COUNT

The gross count extraction method utilizes the integrated counting rate in a single spectral window covering the spectral range.

$$C_{gcw}^{raw} = \left(\frac{1}{t_{live}} \sum_{e=24}^{3066} c(E) \right) \quad \text{EQUATION 1}$$

Where:

- C_{gcw}^{raw} = windowed gross count rate (cps)
- t_{live} = live time during collection of gamma spectrum (s)
- $c(E)$ = count rate for the bin centered on gamma-ray energy e (cps)

HEIGHT ATTENUATION COEFFICIENT MEASUREMENT AND CORRECTION

Advanced data analysis requires the understanding of how the system responds to changes in altitude and requires and understating of background noise in the measured spectra.

Typical background in the gross count window (assumed constant for a complete flight) is removed by first measuring the background over water or high in the atmosphere and subtracting that value from the gross count window. The resulting net count rate is then adjusted to the nominal flight altitude by the following relationship:

$$C_{GC} = (C_{gcw}^{raw} - C_N) e^{\lambda(h-h_0)} \quad \text{EQUATION 2}$$

Where:

- C_{GC} = gross count rate at reference altitude (cps)
- C_N = total count rate attributable to non-terrestrial sources (cps)
- h = actual aircraft (radar measured) altitude (feet or m above ground level)
- h_0 = reference altitude (ft or m)
- λ = effective photon linear attenuation coefficient in air (ft^{-1} or m^{-1})

For this work, the non-terrestrial background count rate, C_N , was determined initially from the high-altitude line (~1000m agl) and adjusted on a flight-by-flight basis, with contributions from cosmic rays, the aircraft system, and airborne radon. It should be noted that the use of an exponential parameterized by a *height attenuation coefficient* for the altitude dependence of the count rate is an empirical approximation. More correct expressions, which explicitly include geometrical effects, use a form of the exponential integral. See, for example, *Gamma Spectrometry of the Natural Environments and Formations* (Kogan, 1971).

DOSE RATE CONVERSION

The C_{GC} can be converted to gamma ray exposure or dose rate by multiplying by a count to dose rate conversion factor (α). This factor is determined empirically by calibrating the response of the spectral system against an instrument that directly reads the desired value. This value can also be determined by Monte Carlo simulation.

$$D_{rate} = \alpha \times C_{GC} \quad \text{EQUATION 3}$$

SPECTRAL EXTRACTION

Window Extractions

The aerial data were also used to determine the location of anthropogenic radionuclides, which are indicated by counts above the continuum in the photo-peak regions of the isotopes of interest. Evidence of anthropogenic radionuclides is sometimes indicated by obvious increases in the gross count rate. However, variations in the gross count do not always indicate the presence of an anthropogenic anomaly. Significant variations can result from geological fluctuations or changes in the ground features (e.g., rivers, dense vegetation, buildings), as well as altitude changes.

Two- and three-window extractions are common methods of determining the count rate in a particular spectral region above background. This work only considers the two-window extraction method. The method compares a lower energy 'photo-peak' region to a higher energy region that is not impacted by the presence of the radiation. The windowed extractions can be expressed analytically in terms of the integrated count rates in specific gamma energy spectral windows:

$$C_{MM} = \sum_{e=a}^b c(E) - K_{MM} \times \sum_{e=c}^d c(E) \quad \text{EQUATION 4}$$

Where:

C_{MM} = anthropogenic count rate at the survey altitude (cps)

$c(E)$ = count rate for the bin centered on gamma-ray energy E

a = start energy or bin of photo-peak

- b = end energy or bin of photo-peak
- c = start energy or bin of high energy region
- d = end energy or bin of high energy region

and

$$K_{MM} = \frac{\sum_{e=a}^b c_{ref}(E)}{\sum_{e=c}^d c_{ref}(E)} \quad \text{EQUATION 5}$$

The K_{MM} ratio is of the low-energy counts to high-energy counts in a background spectrum measured over an area that only contains gamma radiation from naturally occurring radionuclides. Once K_{MM} is determined over clean background, it is treated as a constant for the remaining survey data. $c_{ref}(E)$ represents count rate in the reference gamma-ray energy spectrum at the energy E in cps. This algorithm is sensitive to low levels of anthropogenic radiation even in the presence of large variations in the natural background.

Gaussian Extraction

Gaussian Extractions can also be used to determine the net counts in a photo-peak region of interest throughout survey data. Gaussian extractions may be viewed as an alternative to 2- and 3-window algorithms. Gaussian extractions will be referred to in this document as the process whereby the sum of a continuum and Gaussian response is fit to experimental data, with the Gaussian being subsequently integrated to produce a net photo-peak area (Figure 10). The dominant differences may be summarized as:

- Standard windowing algorithms rely on the ability to define background regions in which it is known that no net isotopic response is present. Gaussian extractions inherently make no such assumption, although care must be taken that background regions are adequately fit with the underlying continuum representation.
- Given environments exhibiting background (relative to isotopic extraction of interest) with constant spectral shape, the standard window mechanisms yield results with optimal statistical properties relative to Gaussian extractions. This is due to a disparity between no degrees of freedom (typical windowing algorithms lock the single degree of freedom that exists), and the several (>3) degrees of freedom exhibited by a Gaussian extraction.
- Gaussian extractions are dramatically (orders of magnitude) more computationally expensive than the standard windowing approaches.
- Gaussian extractions are inherently more robust than windowing algorithms in the limit of infinite count rate – ignoring statistical considerations. This is due to their ability to represent a varying continuum shape.

A simple form of Gaussian extraction may be obtained by fitting a region of spectral response to the summation of a Gaussian and linear underlying continuum as follows:

$$S(E) \approx a + bE + ce \frac{(E - E_0)^2}{2\sigma^2}$$
EQUATION 6

$S(E)$ is the energy dependent raw spectral response, a and b represent the two degrees of freedom associated with a linear continuum, c represents the Gaussian peak height, and the parameters σ and E_0 are the peak standard deviation and centroid values respectively. The parameters σ and E_0 are detector response parameters and are treated as constant.

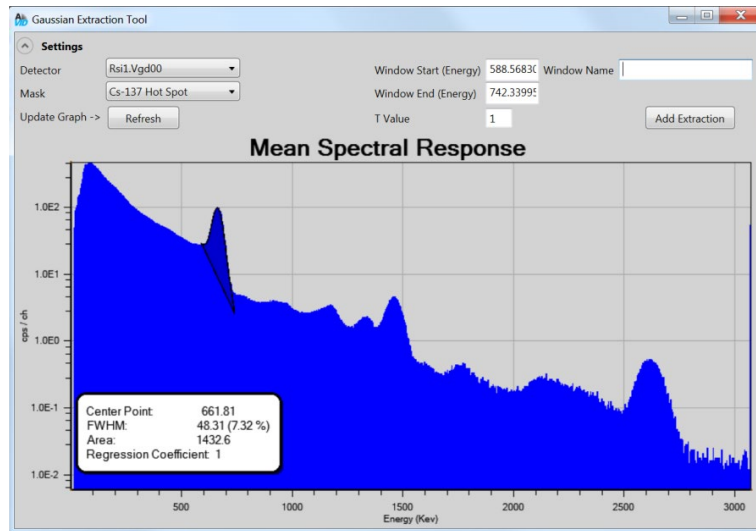


FIGURE 12. EXAMPLE OF THE GAUSSIAN FIT TO CS-137 PEAK IN AVID.

Given a particular fit of the form given by (Eq. 5) the net photo-peak area may be determined simply by integrating the Gaussian to get:

$$I = \frac{\sqrt{2\pi}\sigma c}{\beta}$$
EQUATION 7

The derived net photo-peak area has the same units as the underlying spectrum $S(E)$. The value of β is the energy equivalent of one channel of the histogram response $S(E)$. Alternatively, the spectrum that is fit may be represented in channel space and the value of β becomes one.

DSA/NGU

For post-processing of the data, DSA uses the program RadAssist with the addition of internally authored scripts and add-ons. For map preparation DSA currently uses NGU as a support organization. For this report DSA and NGU have collaborated, where NGU have prepared the data and presented the results in a manner to allow inter-comparison with AMS results.

The spectrometry data collected during this joint mission was provided to NGU by DSA. NGU used Oasis Montaj's Geosoft software to check the data quality and to perform processing of it. Final data as point plots and grids presented here were also prepared using Geosoft.

DATA PREPARATION

Full spectra data were downloaded from RSI acquisition system and converted in ASCII format using RadAssist software by RSI. Full spectra were imported in the database and then counts for various spectral windows were calculated for further processing. The RSX-4 has a GPS inbuilt in the spectrometer. Therefore, we used the spectrometer GPS data for the position of the collected data. The data were processed together with plotting and preparing the maps in Geosoft. Radar altimeter data was not collected by DSA separately therefore we used altitude from in-built GPS of RSX-4 and a digital elevation model (DEM) data with 10 m cell size from <http://ned.usgs.gov/about.html> to estimate flying altitudes above ground. The GPS data was first corrected for geoid height so that altitudes were measured from geoid. Elevations sampled from DEM grids were subtracted from altitudes above geoid to obtain helicopter altitude over surface.

GROSS COUNT AND MAN-MADE GROSS COUNT

NGU has used same Equations 2 & 3 to calculate net gross count (CGC) and anthropogenic/man-made count rates (MMGC or C_{MM}). NGU used gamma-ray energies of 24 keV and 3045 keV for Equation 2. Gamma energies of 24, 1395, 1395 and 3045 keV were used for a, b, c and d respectively for Equations 3 & 4. DSA had mounted its RSX-4 system inside the helicopter and therefore it was shielded by the helicopter body. However, AMS had its 4 pods (12 crystals of 2 liters each, total 24 liters) mounted outside at left and right side of the helicopter (described in section 'Aerial measuring system'). Therefore, values of C_{GC} will be different to AMS values. Dose rates parameters were calculated by NGU for DSA data in same way as done by AMS against a measured exposure/ dose rate. Therefore, dose rate ranges from different locations will be in close agreement from both AMS and DSA/NGU data.

INDIVIDUAL NUCLIDES IDENTIFICATION

NGU didn't use two-window or Gaussian method for individual nuclides, but it looked through various nuclides window (a small window around the peak of possible nuclides) for all the areas. The nuclides present in the area could have back scattered gamma rays in lower energy windows of other nuclides as well. We assume that back-scattered counts would be relatively less than the window counts of the present nuclides (which is not true in some cases e.g., Cs-137 window has back scattered contribution of U and Th decay elements i.e., Bi-214 and Tl-208, respectively). Therefore, distribution of window counts for the nuclides which were not present in the area would be relatively homogenous without any anomalous regions than for the nuclides which were present.

GRIDDING/CONTOURING AND COLOR SCALES

NGU gridded all data in Oasis Montaj from Geosoft using minimum curvature. NGU created a similar color scheme in Oasis Montaj as used by AMS for the plotting. AMS has used a natural breaks (jenks) color scale however, NGU has used a linear color scale because Oasis Montaj does

not have natural breaks color scale. The use of different color scales is also one of the main reasons (other than different shielding and processing technique for individual elements) that we cannot see the exact same patterns in the plots from AMS and NGU images but nonetheless they will show some similarity.

ORGANIZATION OF THE CAMPAIGN

JOINT SURVEY ACTIVITY PLAN

As a normal part of previous operations, several areas in Southern Nevada and the NNSS were chosen as survey locations. The operations plan included flights over the AMS calibration ranges at Government Wash and Lake Mohave, and survey flights over Areas 3, 8 & 10, 11, and 30 at the NNSS. Each day the aircraft took off from Nellis Air Force Base and transited to Desert Rock Airport (DRA) at the NNSS. During the series of surveys, AMS personnel also held a course in advanced AMS data processing for a larger international audience.

DESCRIPTION OF SURVEY SITES

GOVERNMENT WASH

Government Wash is located 10 miles (16 km) east of RSL and is characterized by varied geology. AMS has used this location for evaluation of responses of aerial acquisition systems to varied natural background for many years (Figure 11). The survey area is approximately 3 square miles (8 km²).

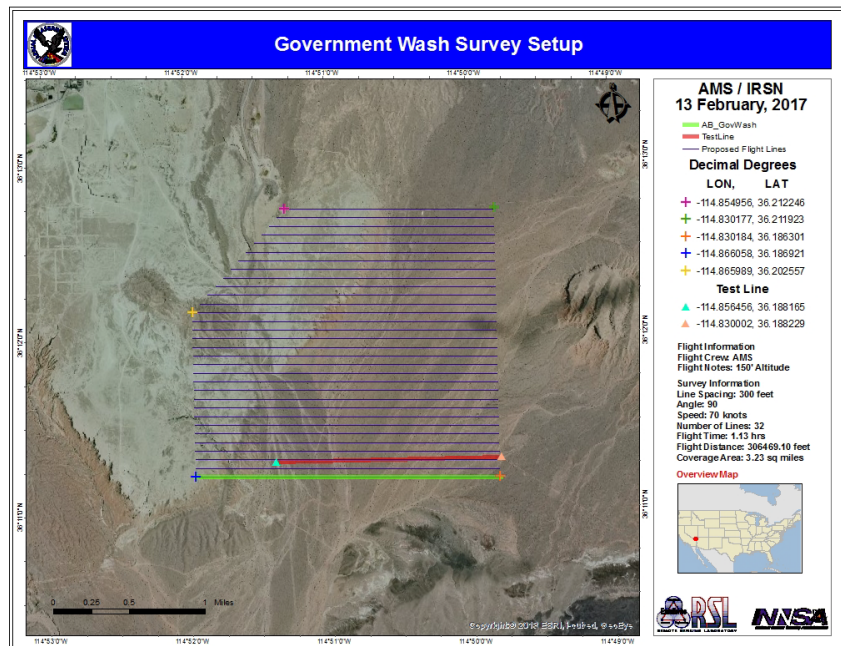


FIGURE 13. PROPOSED SURVEY SETUP AT THE GOVERNMENT WASH SITE.

LAKE MOHAVE CALIBRATION RANGE

Since 1995, the Lake Mohave Calibration Range (LMCR) has been used by AMS as an environmental reference standard flight line to monitor and verify the integrity of AMS acquisition systems. The LMCR is located approximately 0.6 mi (1 km) west of the western shoreline of Lake Mohave, Nevada, and 12.4 mi (20 km) east of Searchlight, Nevada (Figure 12). The land calibration line at LMCR is approximately 2.8 mi (4.6 km) long with elevation variations along the test line between 780 ft (240 m) to 960 ft (290 m) mean sea level (MSL).

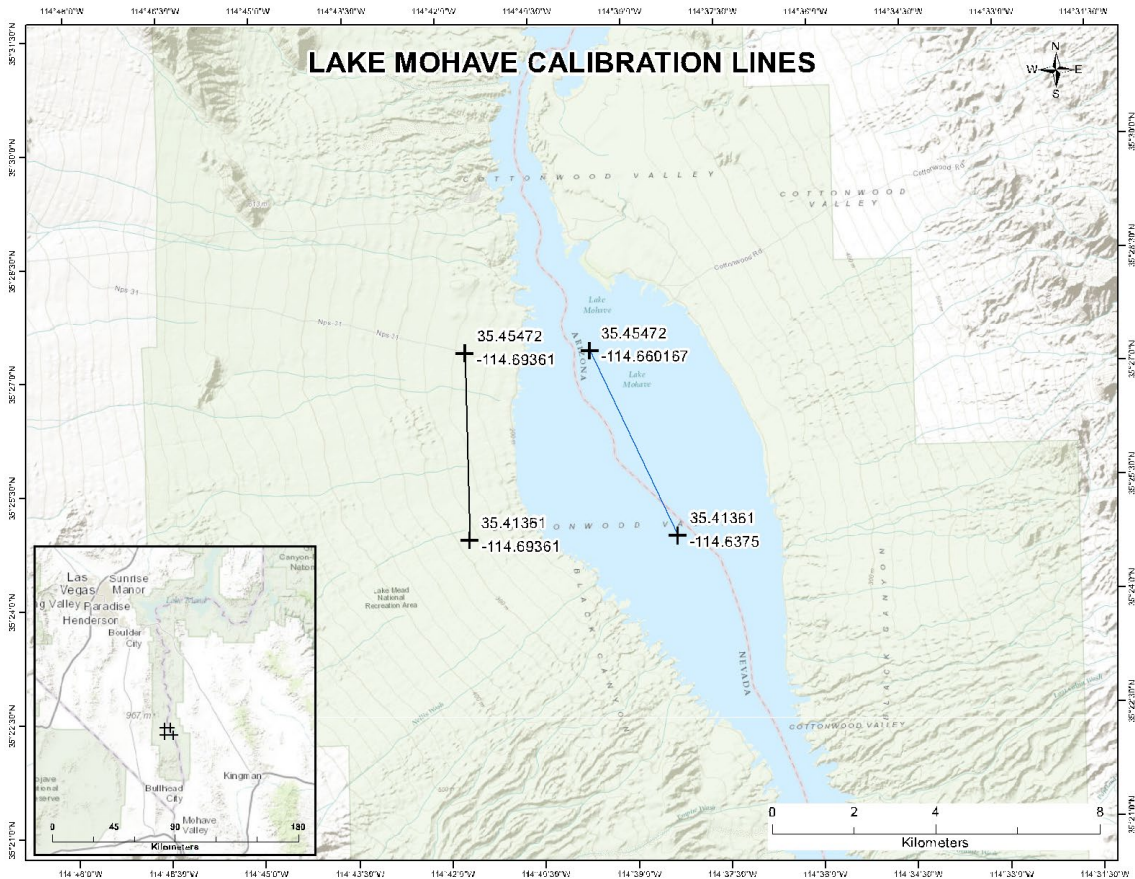


FIGURE 14. THE LAND AND WATER CALIBRATION LINES AT THE LAKE MOHAVE CALIBRATION RANGE.

NEVADA NATIONAL SECURITY SITE

Starting in January 1951, the Nevada National Security Site (NNSS), formerly the Nevada Test Site, became the primary U.S. site for testing nuclear weapons and for studying their effects on structures and military equipment. The NNSS is located approximately 65 mi (105 km) northwest of Las Vegas. It covers an approximately 1,350 mi² (~3500 km²) area. The elevation above MSL ranges from ~2,690 ft (~809 m) to ~7,680 ft (~2340 m).

In this joint exercise, surveys were flown at five areas:

Area 3 was the location of several tests. In the southern portion, Fizeau was detonated on a tower on September 14, 1957, with a yield of 11 kt. The central portion hosted two tests conducted from towers: Harry (May 19, 1953; 32 kt) and Hornet (March 12, 1955; 4 kt). Also, in this immediate area were two other test locations: Coulomb-A (July 1, 1957; 0 kt), a safety experiment conducted at ground level, and Rio Arriba (October 18, 1958; 0.09kt) on a tower. The AMS 1994 (Hendricks & Riedhauser, 1999) survey located five regions of anthropogenic activity. The three main test areas all contained ⁶⁰Co, ¹³⁷Cs, ¹⁵²Eu, and ²⁴¹Am.

Area 11 (Pu Valley) is the site of four safety experiments that occurred during November 1955 through January 1956. The four safety experiment locations have identifiable amounts of ²⁴¹Am.

Areas 8 and 10 are the location of the Sedan test. Sedan was a Plowshare test conducted on July 6, 1962, with a yield of 104 kt. This excavation experiment created a crater with a depth of 320 ft and a diameter of 1280 ft. The test resulted in the release of radioactivity that was detected off-site. The spectrum of this region contained ⁶⁰Co, ⁶⁵Zn, and ¹³⁷Cs.

Area 30 is the location of the Buggy test, which included simultaneous detonations on March 12, 1968, as part of the Plowshare program. The purpose of the test was to assess the ability to carve a channel through the ground using nuclear devices. Each of the five devices produced a published yield of 1.08 kt. As at the Sedan location, the identified isotopes at Area 30 were ⁶⁰Co, ¹³⁷Cs, ²⁴¹Am. This area was of particular interest for its topography with the test having taken place on a plateau surrounded by deep canyons.

Historical operations in these areas resulted in contamination consistent with that of a nuclear/radiological accident/incident with different types and amounts of dispersed radioactive materials. The locations of the survey areas at the NNSS are presented in Figure 13. For the AMS/DSA joint survey the planned flight parameters included flight altitude of 150 feet (46 m) AGL, line spacing of 300 feet (91 m) and an aircraft speed of 36m/s (70 knots), except for Area 11 where an altitude of 50 feet (15 m) and line spacing of 100 feet (30 m) were planned. The survey areas selected for the joint survey provided a variety of radionuclides in the ground contamination, which created a test bed for both teams to carry out spectral analyses of collected data.

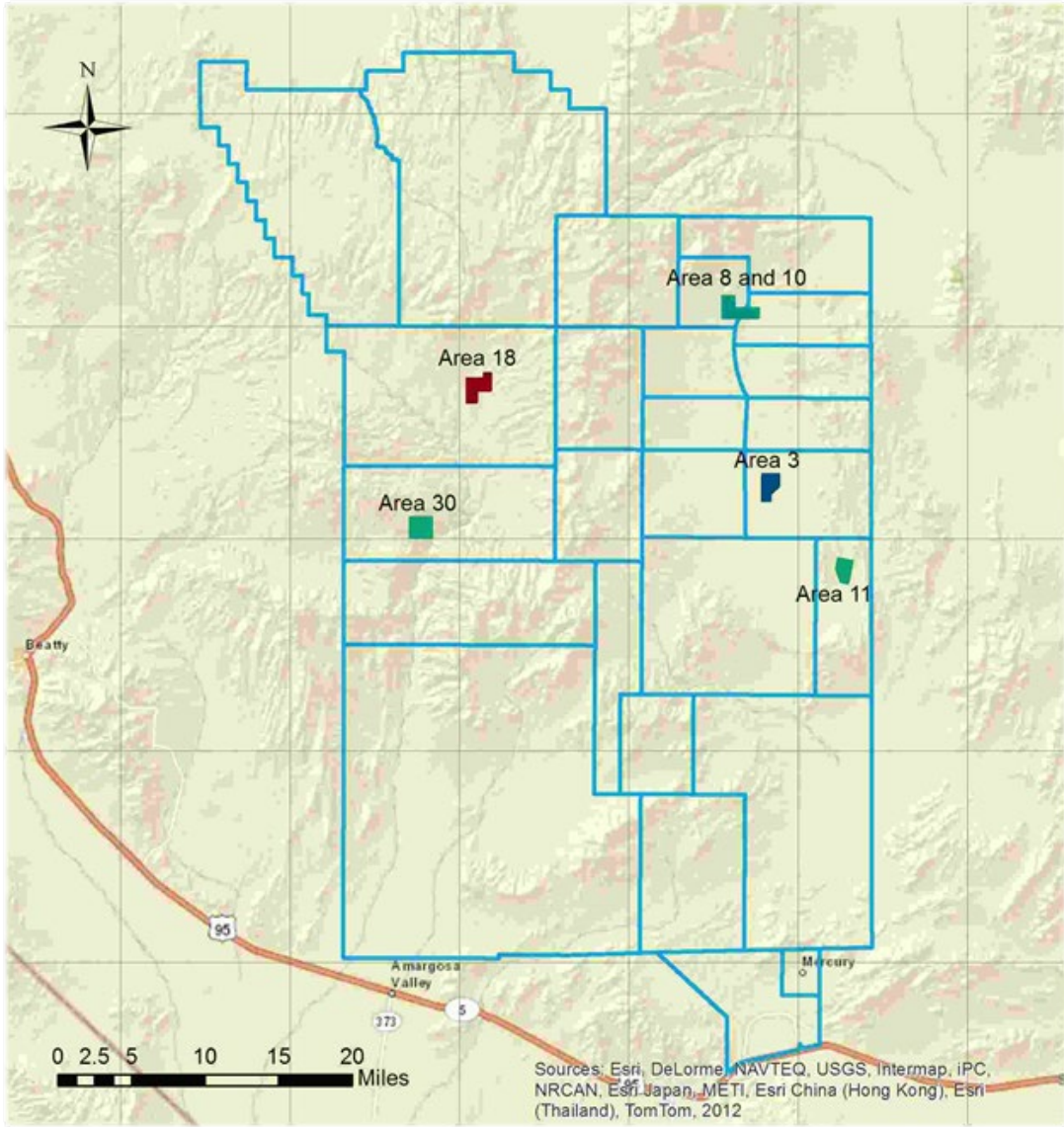


FIGURE 15. LOCATIONS OF COMMON SURVEY AREAS AT THE NNSS.

AMS AND NGU RESULTS

ATTENUATION AND SENSITIVITY

LAKE MOHAVE CALIBRATION RANGE

The flight over the calibration line at the Lake Mohave Calibration Range includes lines over land and water at the same nominal altitude (Figures 14 & 15 from AMS and Figures 16 & 17 from NGU). They were used to calibrate the system against historical ground measurements in terms of exposure rate in microRoentgen per hour ($\mu\text{R/h}$), and to determine the local height attenuation coefficient. Altitudes used in this campaign were 15, 50, 150, 300, 500 and 1000 m AGL.

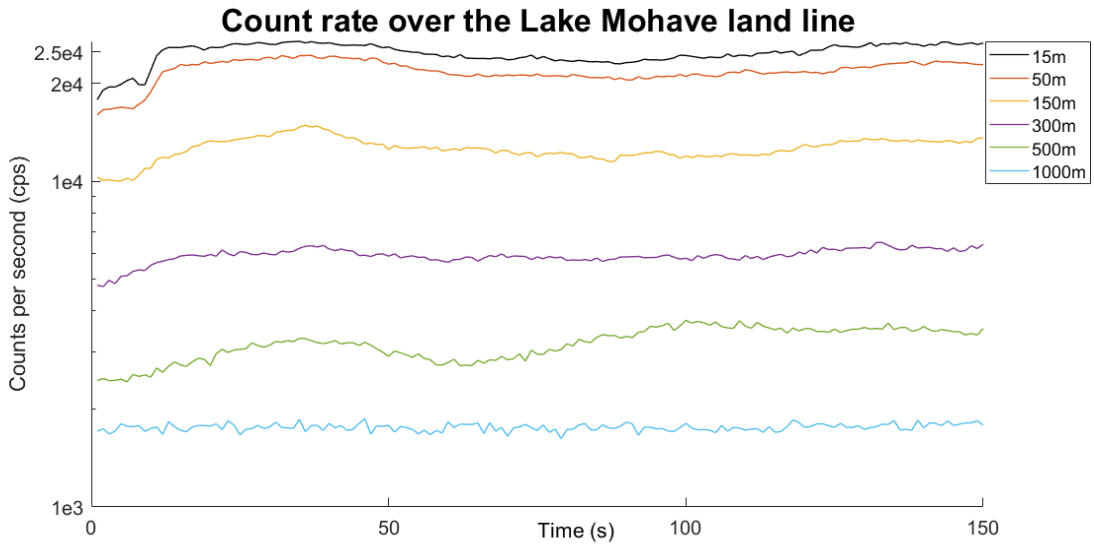


FIGURE 16. GROSS GAMMA COUNT RATE TIME SERIES OVER THE LAND CALIBRATION LINE FOR THE AMS SYSTEM.

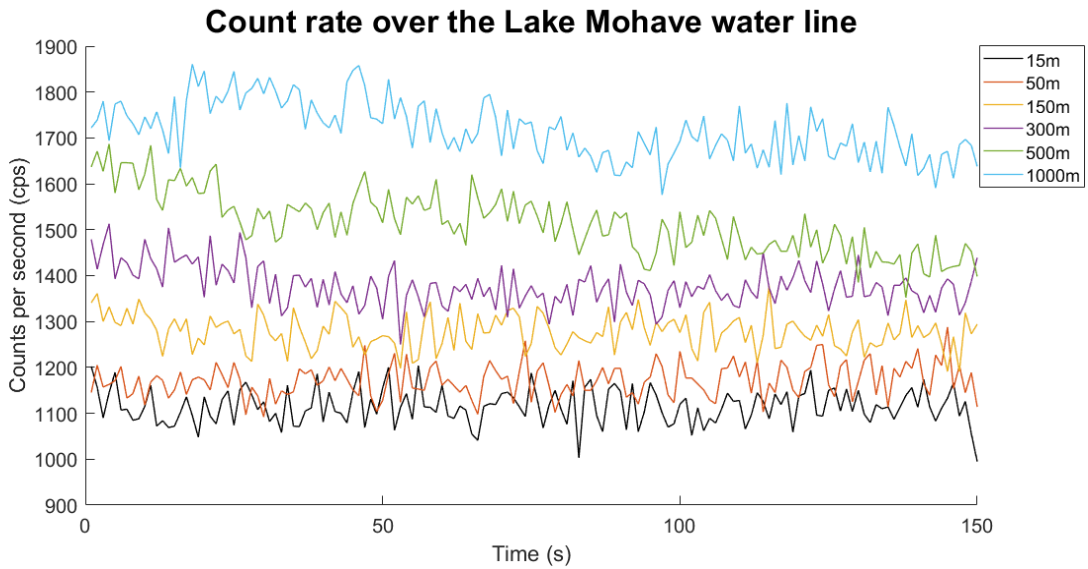


FIGURE 17. GROSS GAMMA COUNT RATE TIME SERIES OVER THE WATER LINE FOR THE AMS SYSTEM.

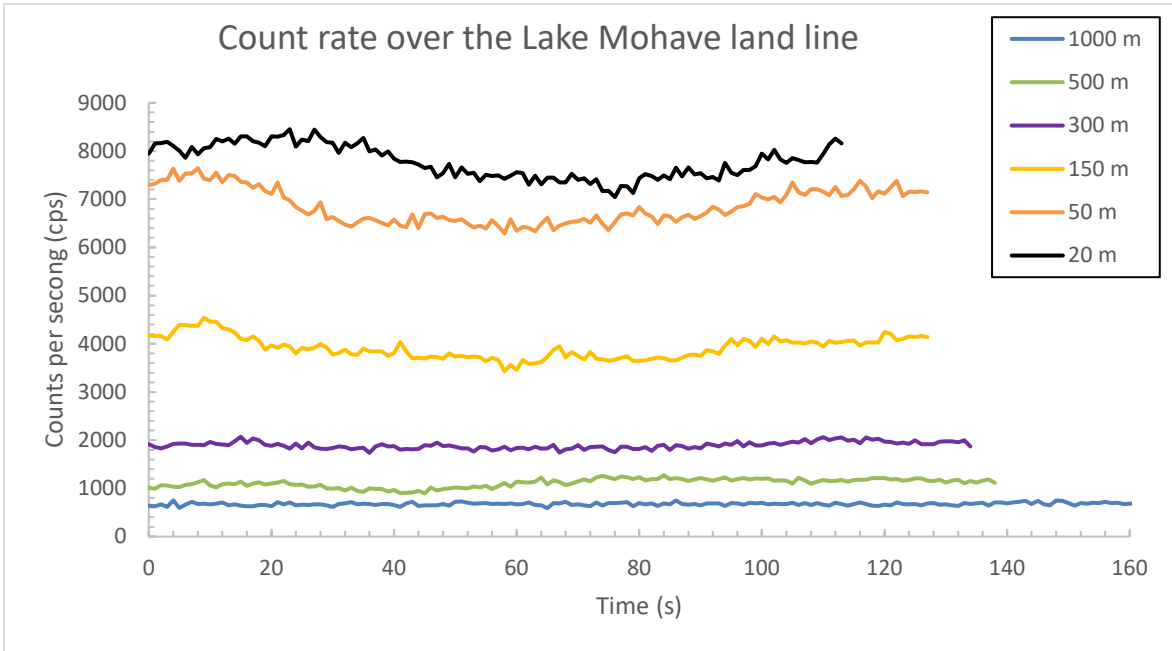


FIGURE 18. GROSS GAMMA COUNT RATE TIME SERIES OVER THE LAND LINE FOR THE DSA SYSTEM PLOTTED BY NGU.

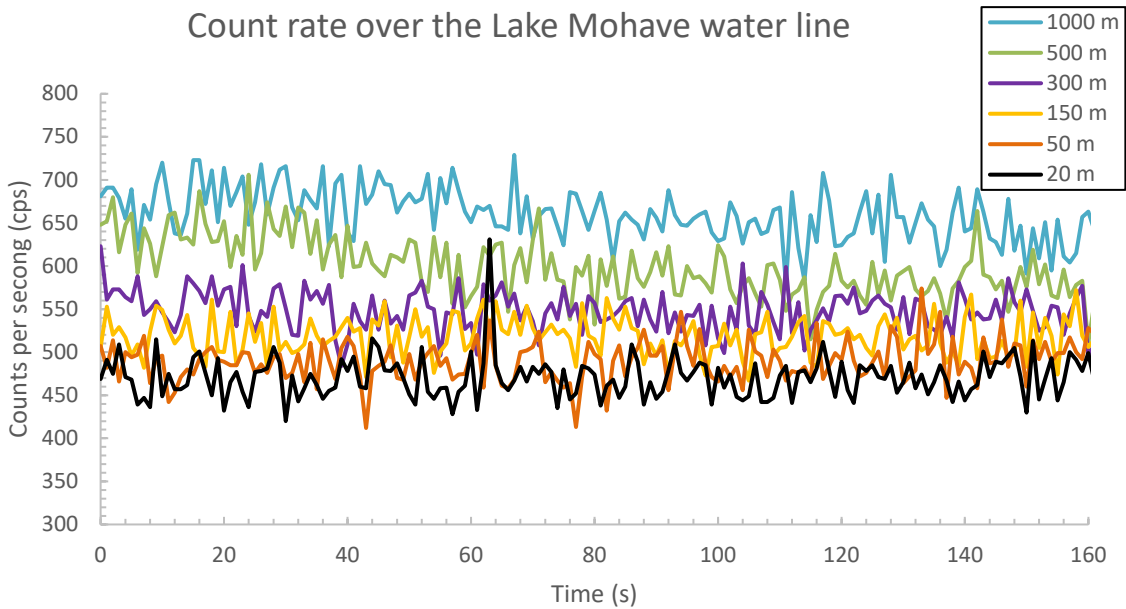


FIGURE 19. GROSS GAMMA COUNT RATE TIME SERIES OVER THE WATER LINE FOR THE DSA SYSTEM PLOTTED BY NGU.

From the average count rates recorded over the calibration line, the AMS & DSA system count rate exhibits (Table 1 & 2 and Figures 18 & 19) an exponential dependence on altitude and yielded

a local height attenuation coefficient as reported in Table 3. In addition, DSA provided AMS with their data. The height attenuation coefficient for DSA's data as determined by AMS is also found in Table 3. NGU has calculated this coefficient for DSA data and provided in Table 3.

TABLE 1. AVERAGE GROSS COUNT RATES FROM AMS DETECTOR SYSTEM AT THE CALIBRATION LINE.

NOMINAL AND AVERAGE ALTITUDE [METERS AGL]	LAND [CPS]	WATER [CPS]
15 (19)	24880	1115
50 (43)	21950	1173
150 (148)	12664	1276
300 (302)	5942	1374
500 (471)	3195	1510
1000 (924)	1760	1705

*ALTITUDE DATA DERIVED FROM GPS POSITION AND CORRECTED USING THE NED 10 DIGITAL ELEVATION MODEL.

TABLE 2. AVERAGE GROSS COUNT RATES CALCULATED BY NGU FROM DSA DETECTOR SYSTEM AT THE CALIBRATION LINE.

NOMINAL AND AVERAGE ALTITUDE [METERS AGL]	AVERAGE LAND [CPS]	AVERAGE WATER [CPS]
20 (21)	7565	471
50 (56)	6888	490
150 (173)	3909	518
300 (319)	1883	547
500 (481)	1093	595
1000 (931)	674	658

*ALTITUDE DATA DERIVED FROM GPS POSITION AND CORRECTED USING THE NED 10 DIGITAL ELEVATION MODEL.

+WATER LINE COUNTS FIT TO A CURVE TO APPROXIMATE VALUE AT LAND ALTITUDE.

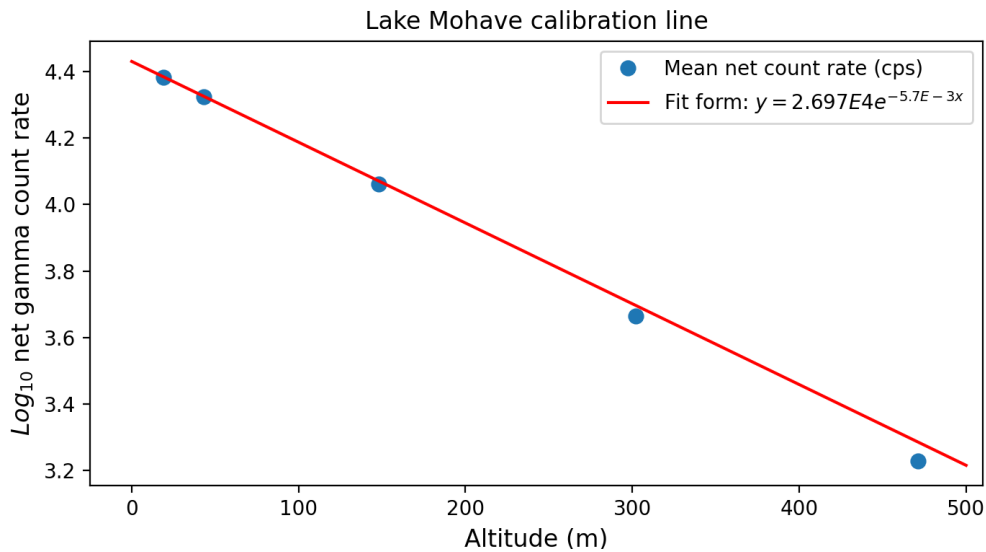


FIGURE 20. LOG PLOT OF NET GAMMA COUNTS VS ALTITUDE USED TO CALCULATE HEIGHT ATTENUATION.

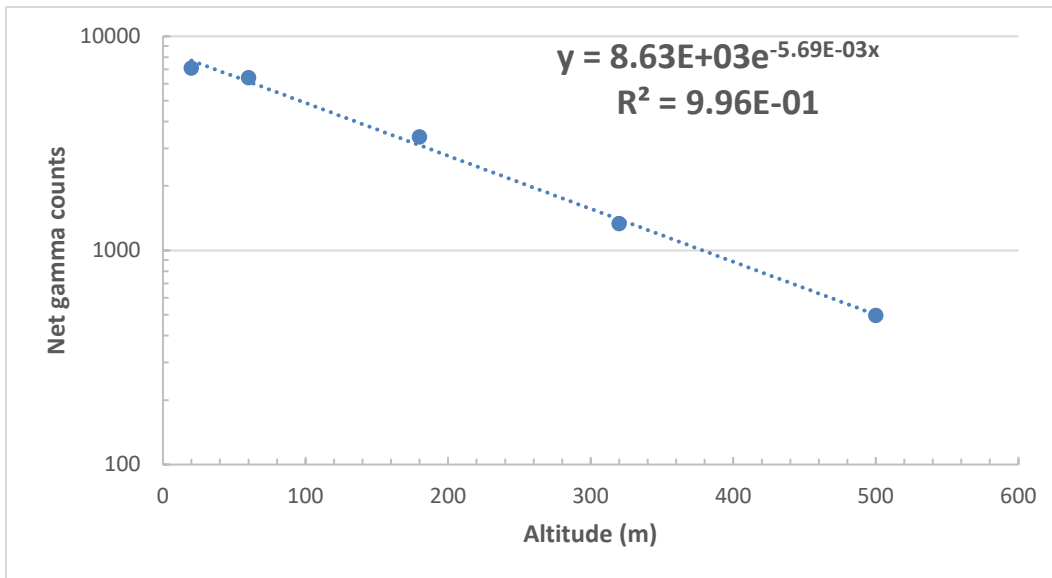


FIGURE 21. LOG PLOT OF AVERAGE NET GAMMA COUNTS VS ALTITUDE USED TO CALCULATE HEIGHT ATTENUATION BY NGU.

Once the data are background subtracted for non-terrestrial sources and scaled to 1 meter above the ground, they are calibrated to previously obtained ground measurements taken at Lake Mohave. The ground measurements determined an average natural background of 8.5 $\mu\text{R}/\text{h}$ after the subtraction of radon and cosmic radiation. This produced a count to exposure rate conversion factor in terms of $\mu\text{R}/\text{h}/\text{cps}$ (Table 3). DSA's data as processed by AMS and NGU are also found in Table 3.

TABLE 3. HEIGHT ATTENUATION AND COUNT TO EXPOSURE RATE COEFFICIENTS (DSA DATA CALCULATED BY AMS).

Asset	Height attenuation coefficient (m ⁻¹)	CPS to Exposure Rate (μR/h/cps)	CPS to Exposure Rate (scaled to 1 crystal)
AMS	5.7e-3	3.37e-4	4e-3
DSA (by AMS)	5.72e-3	1.04e-3	4.16e-3
DSA (by NGU)	5.69e-3	1.04e-3	4.16e-3

SPECTRAL EXTRACTIONS

Spectral extractions were also performed using the methods outlined in the Data Evaluation Methods of this report. Several isotopes were identified by referring to previous work (Hendricks et al.) and by gamma spectroscopic methods. The primary isotopes of interest are: Am-241, Co-60, Eu-152, and Cs-137. In the Government Wash area, the elements of interest are those found in natural background: K, U, and Th.

The windows used for the extractions are found in Table 4 along with the method of extraction. The IAEA method for extracting K, U, and Th are described in the IAEA Technical Document (IAEA, 2003).

TABLE 4. EXTRACTION WINDOWS AND METHODS.

Extraction	Window A (keV)	Window B (keV)	Method
Gross Counts	24-3066	-	One Window
Am-241	40-75	78-100	Two Window
Eu-152	760-1100	1500-3000	Two Window
Co-60	1160-1350	1500-3000	Two Window
Cs-137	585-741	-	Gaussian
K	1370-1570	-	IAEA
U	1660-1860	-	IAEA
Th	2410-2810	-	IAEA

Two-window extraction methods also require a locally measured normalization value, referred to as a k value (Table 5). The k value is measured by referring to the data collected in a known background area and applied to the data of interest. In the case of the data collected during this survey, AMS used the data collected over DRA to determine this value. While the same location was used for each area, radon levels in the atmosphere at the time of collection affect the value by changing the overall spectral shape. Therefore, the same isotope in different areas may have a different k value despite having been measured at the same location. It should also be noted that these values have been determined at a location that is a significant distance from the areas of interest. A more rigorous approach would require a background flight near each area of interest. However, due to the extensive contamination levels at the NNSS, and the additional time requirements involved, it was determined that the DRA data would serve well for these extractions while also serving as a quality control check on the data.

TABLE 5. K VALUES DETERMINED FOR VARIOUS ISOTOPES FOR EACH AREA.

Area	Isotope	k
Area 8	Am-241	1.44375
	Eu-152	3.81115
	Co-60	0.77
Area 30	Am-241	1.31
	Eu-152	1.75
	Co-60	0.534
Area 11	Am-241	1.33
	Eu-152	1.72
	Co-60	0.49
Area 3	Am-241	1.44375
	Eu-152	3.811147
	Co-60	0.77

K_{MM} (Equation 5) for Man-made gross counts (MMGC, C_{MM}) using two-window method was calculated to be 18.65 for DSA data by NGU from government wash area.

NGU followed a spectral window extraction method to remove Compton background described by (Oberlercher & Seiberl, 1997) and (Thørring, et al., 2019) for Cs-137 with slight modification. The Compton background (Figure 20) was subtracted from Cs-137 window counts as shown in Equation 8. The same approach to remove the Compton background for other nuclides with different gamma-rays windows was followed for Am-241, Co-60 and Eu-152 from Area 3, 8, 11 and 30 and K, U and Th from Government wash area. Spectral windows used by NGU for the various nuclides are shown in Table 6.

$$C_S^{Corrected} = \frac{C_S^{WindowCounts} - C_S^{Compton}}{C_S^{WindowChannels}}$$

EQUATION 8

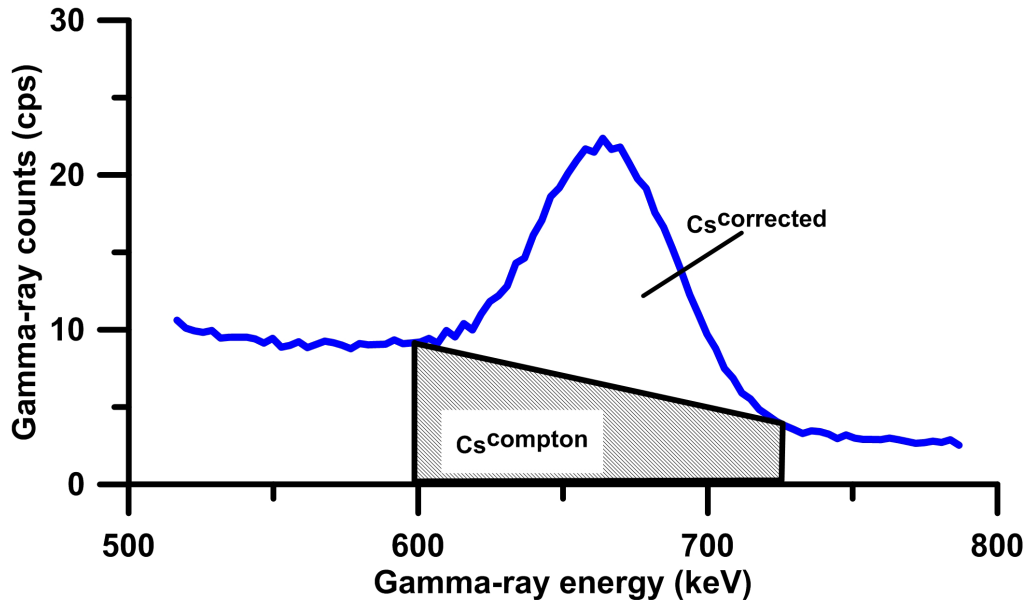


FIGURE 22. COMPTON BACKGROUND CORRECTION.

TABLE 6. EXTRACTION WINDOWS FOR NGU.

Extraction	Window A (keV)	Window B (keV)	Method
Gross Counts (C_{GC})	24-3045	-	One Window
Man-made counts (C_{MM})	24-1395	1401-3045	Two Window
Am-241	45-66	-	Spectral window
Eu-152	930-1000	-	Spectral window
Co-60	1160-1350	-	Spectral window
Cs-137	600-720	-	Spectral window
K	1370-1570	-	IAEA
U	1660-1860	-	IAEA
Th	2410-2810	-	IAEA

DATA PRODUCTS

PRODUCT PRESENTATION

The calibration performed at the Lake Mohave calibration range yielded a conversion coefficient in terms of exposure rate (\dot{X}) with units of microRoentgen per hour ($\mu\text{R/h}$). This is because the pressurized ion chamber used to calibrate the aerial data directly measures radiation exposure in terms of Roentgen. The data products that are presented in terms of Sieverts assume a factor of 100 between the Roentgen and Sievert.

The spectral extraction products are typically presented as counts above background in the spectral region of interest. Because this report intends to compare systems of different volumes and efficiencies, these data are instead represented in terms of standard deviations of the counts above background in the spectral region of interest. The spectral extraction products for separate nuclides are presented in the appendix. NGU has also calculated and prepared man-made gross counts (MMGC or C_{MM}) and presented it in the appendix. NGU has shown Compton background removed nuclides spectral window.

NATURAL BACKGROUND AT GOVERNMENT WASH

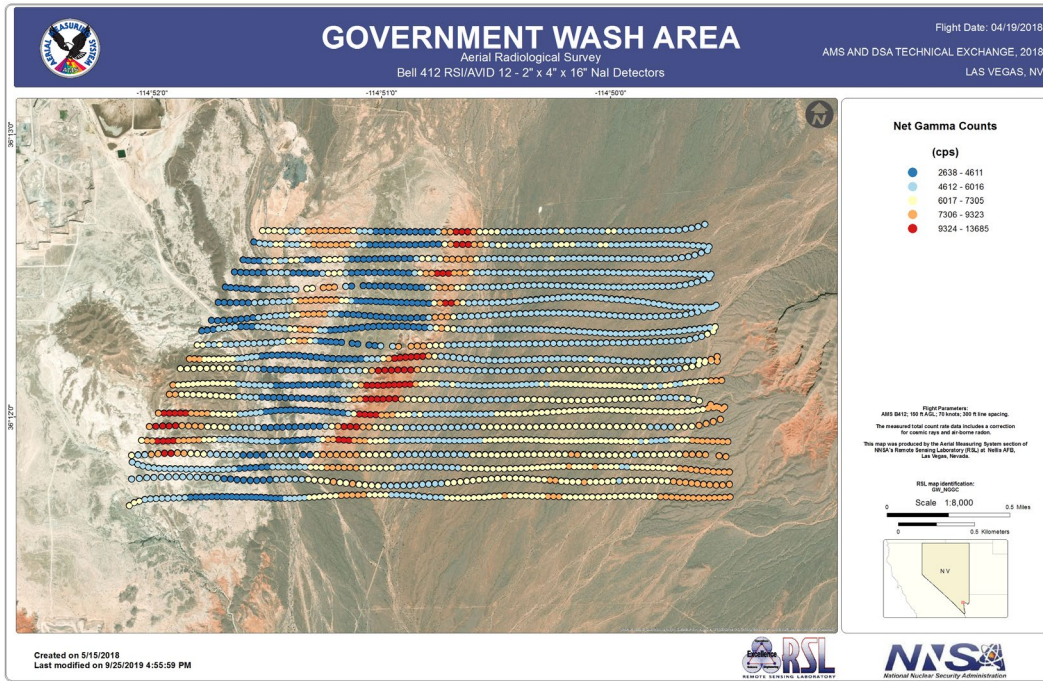


FIGURE 23. GROSS COUNT OF THE NATURAL BACKGROUND AREA (GOVERNMENT WASH) FROM AMS DATA.

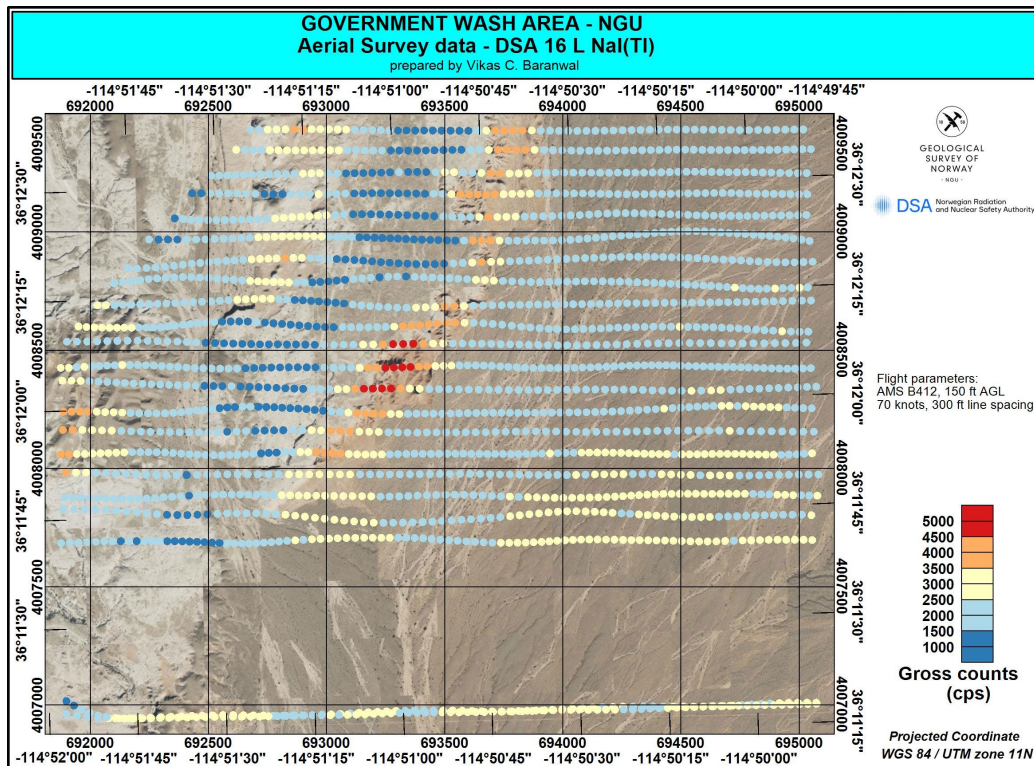


FIGURE 24. GROSS COUNTS OF THE NATURAL BACKGROUND AREA (GOVERNMENT WASH) FROM DSA DATA.

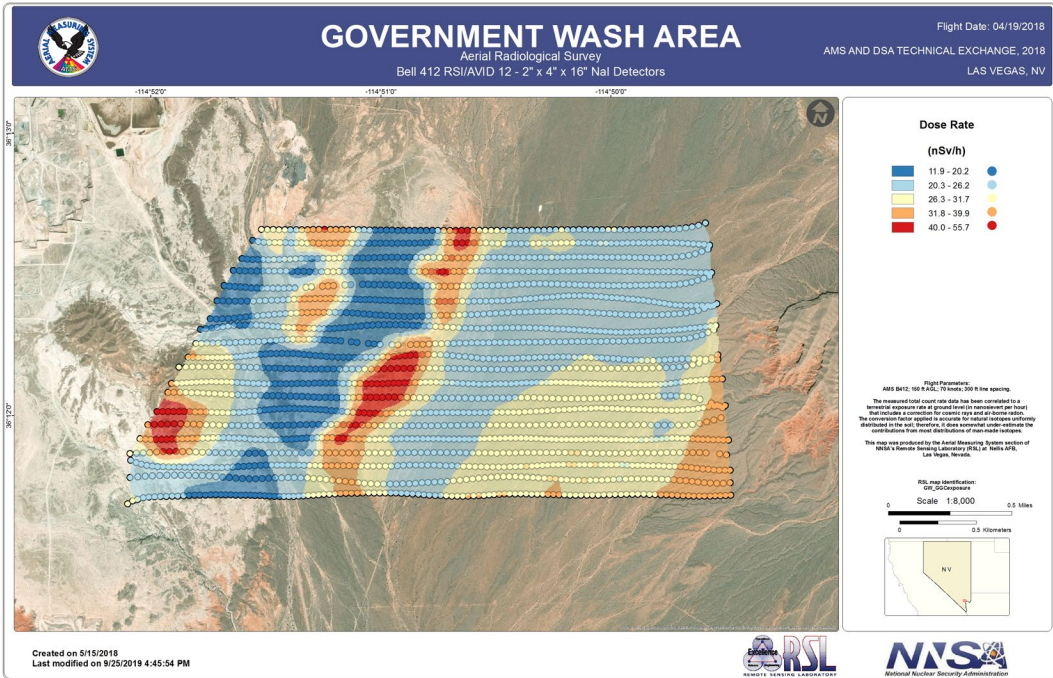


FIGURE 25. DOSE RATE OF THE NATURAL BACKGROUND AREA (GOVERNMENT WASH) FROM AMS DATA.

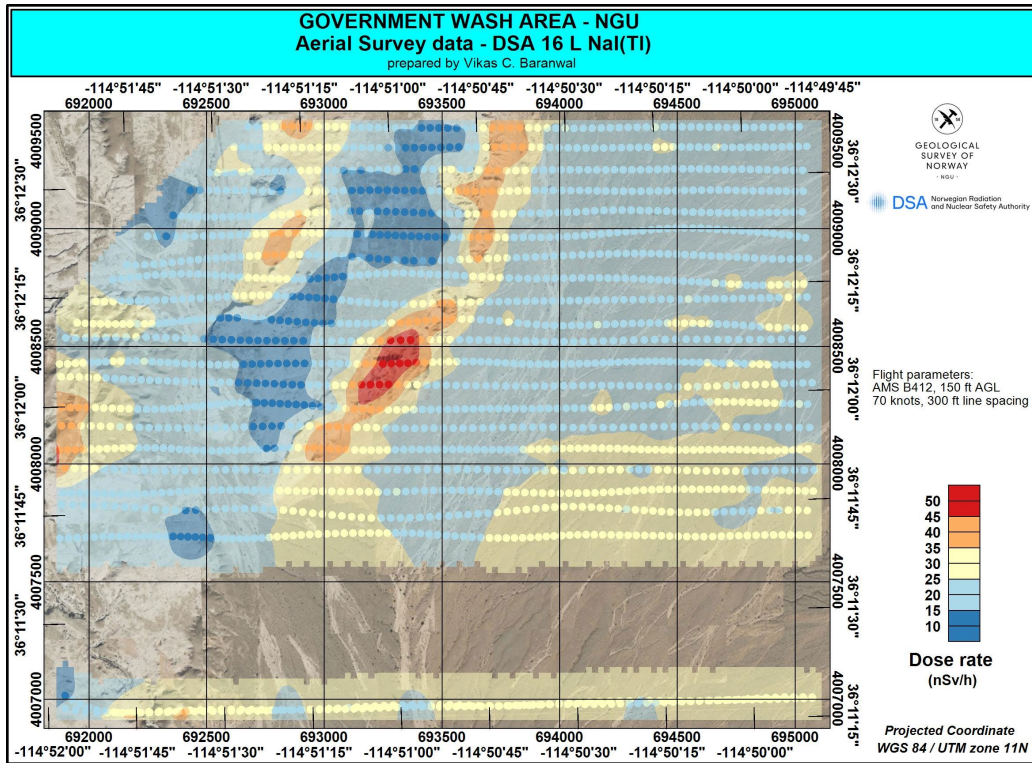


FIGURE 26. DOSE RATE OF THE NATURAL BACKGROUND AREA (GOVERNMENT WASH) FROM DSA DATA.

NNSS AREA 3

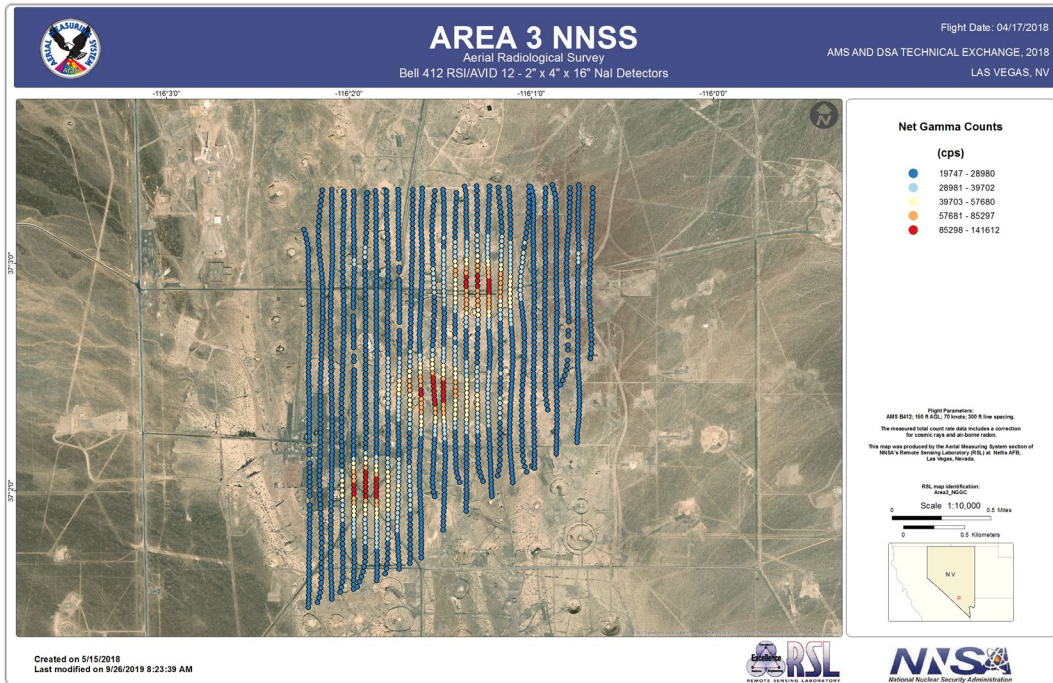


FIGURE 27. GROSS COUNTS FROM NNSS AREA 3 FROM AMS DATA.

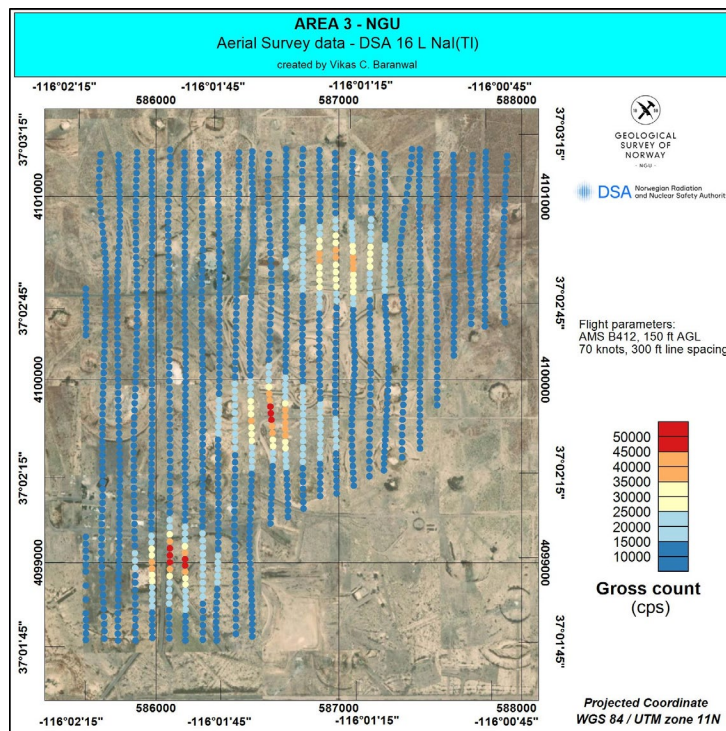


FIGURE 28. GROSS COUNTS FROM NNSS AREA 3 FROM DSA DATA.

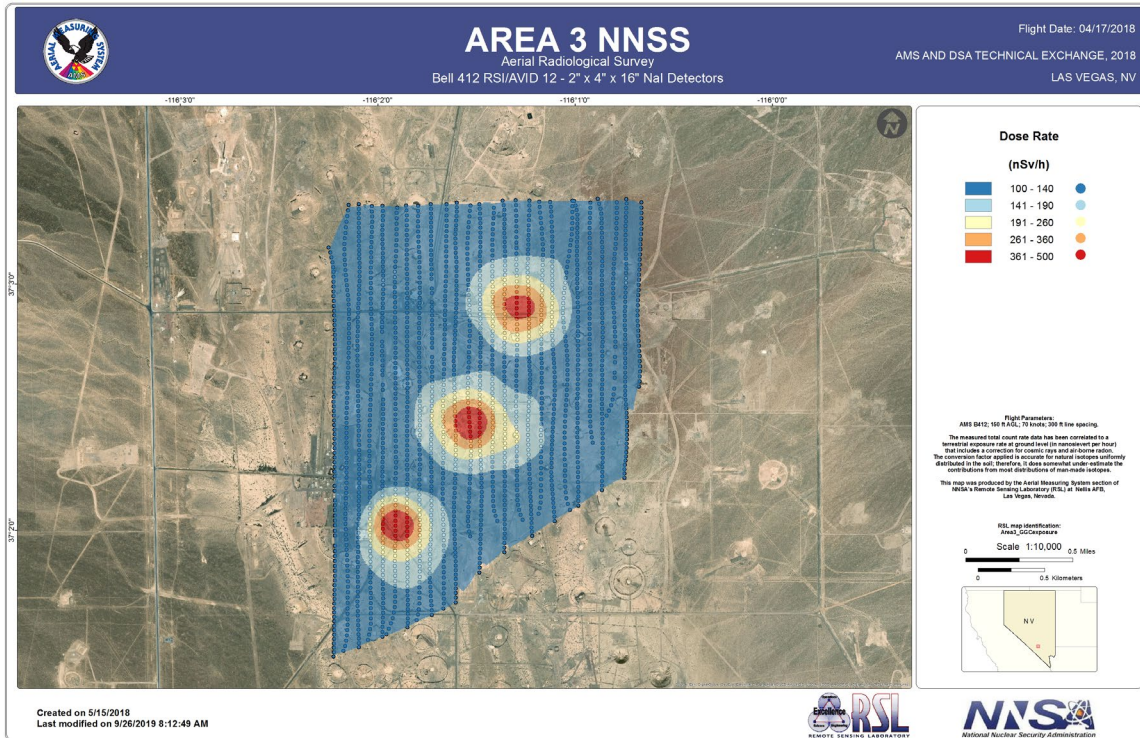


FIGURE 29. DOSE RATE FROM NNSS AREA 3 FROM AMS DATA.

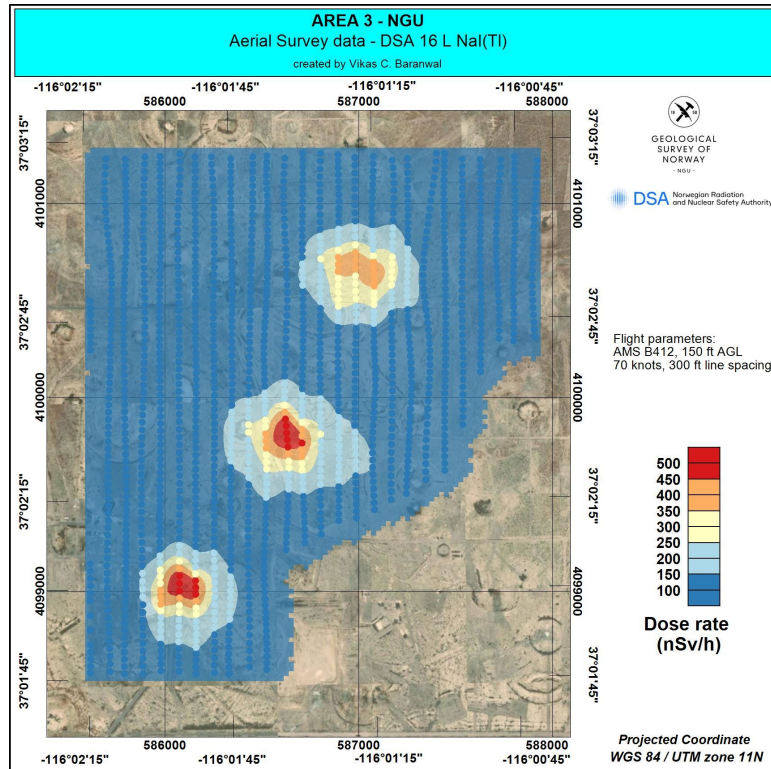


FIGURE 30. DOSE RATE FROM NNSS AREA 3 FROM DSA DATA.

NNSS AREA 8

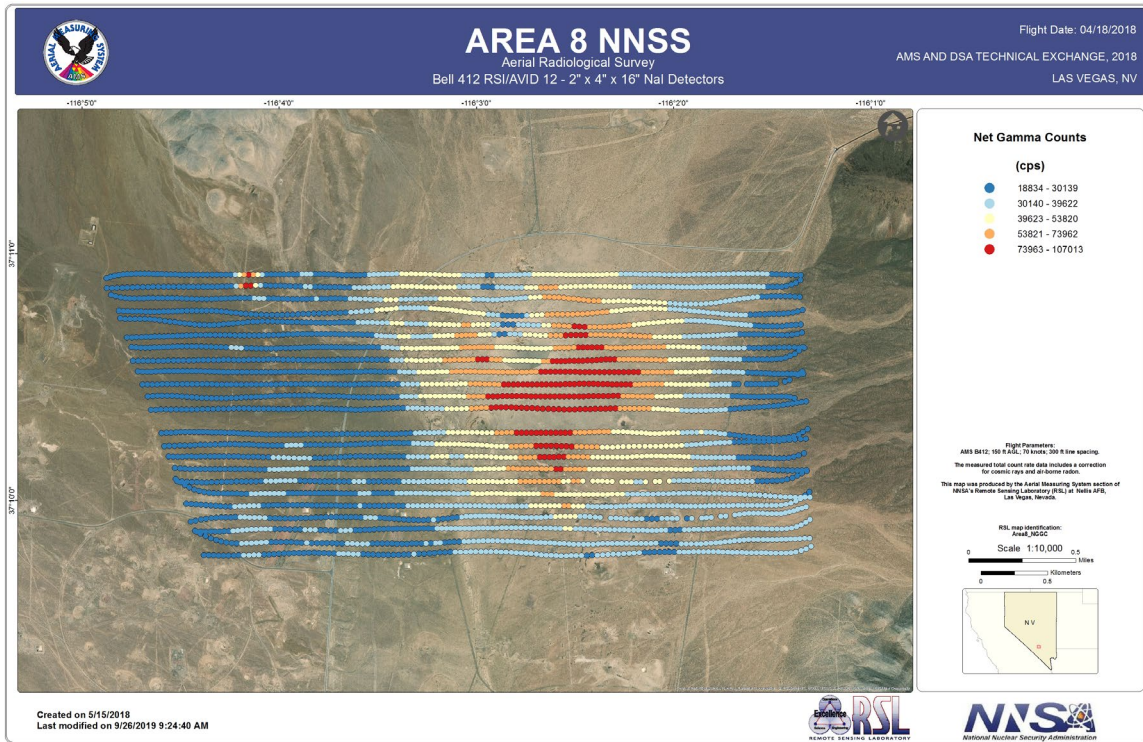


FIGURE 31. GROSS COUNTS FROM NNSS AREA 8 FROM AMS DATA.

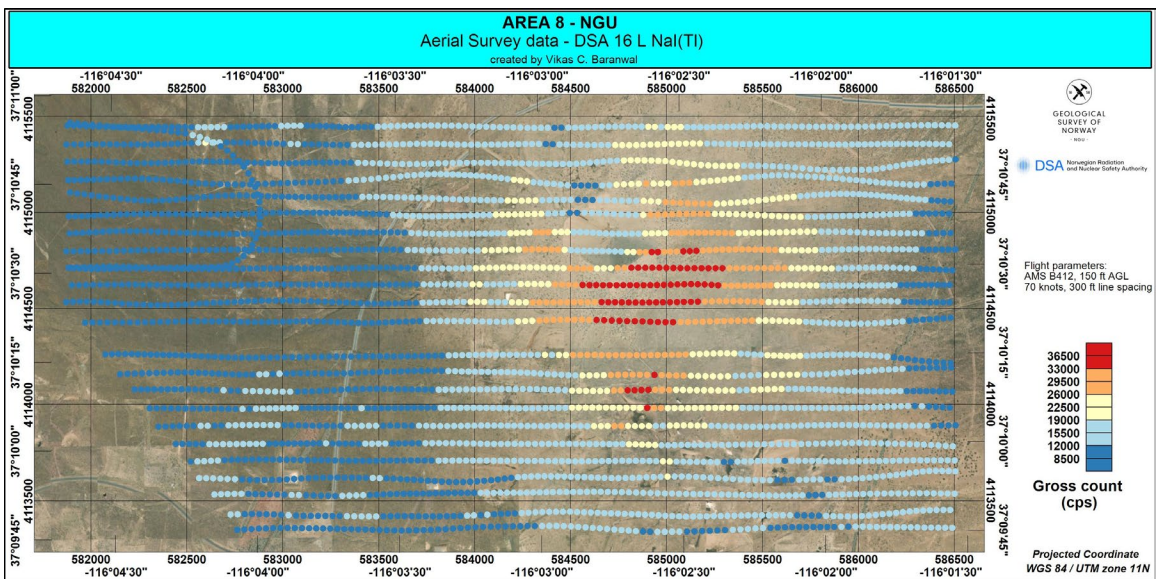


FIGURE 32. GROSS COUNTS FROM NNSS AREA 8 FROM DSA DATA.

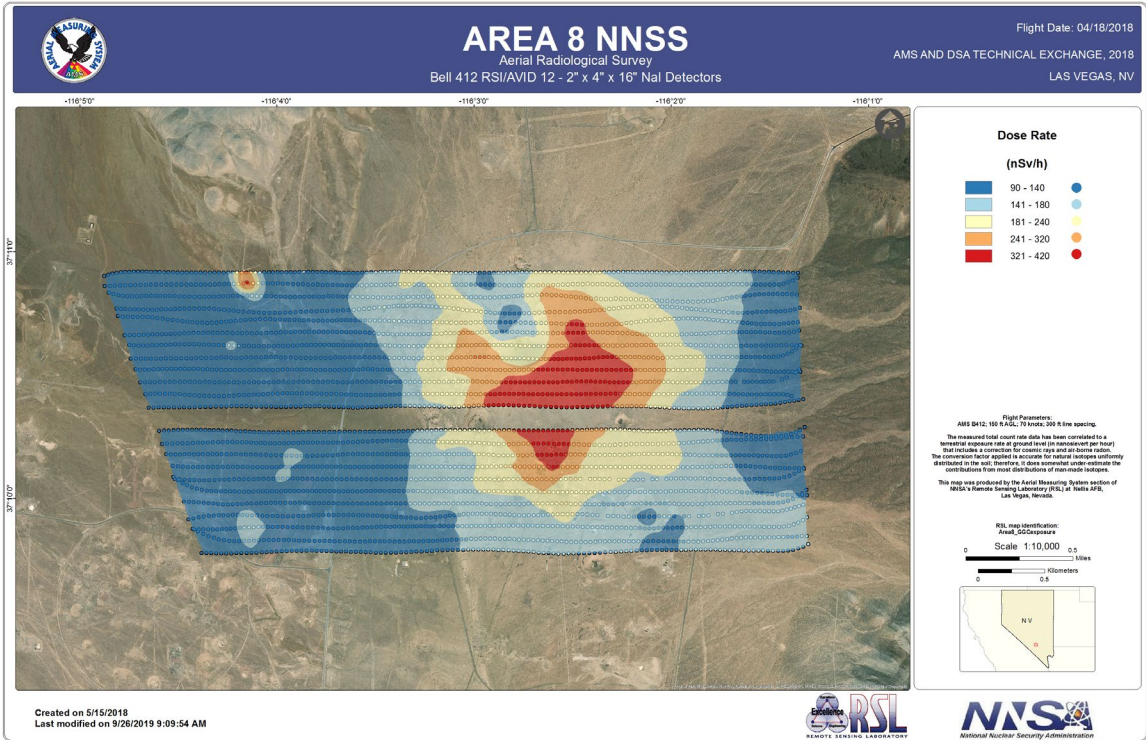


FIGURE 33. DOSE RATE FROM NNSS AREA 8 FROM AMS DATA.

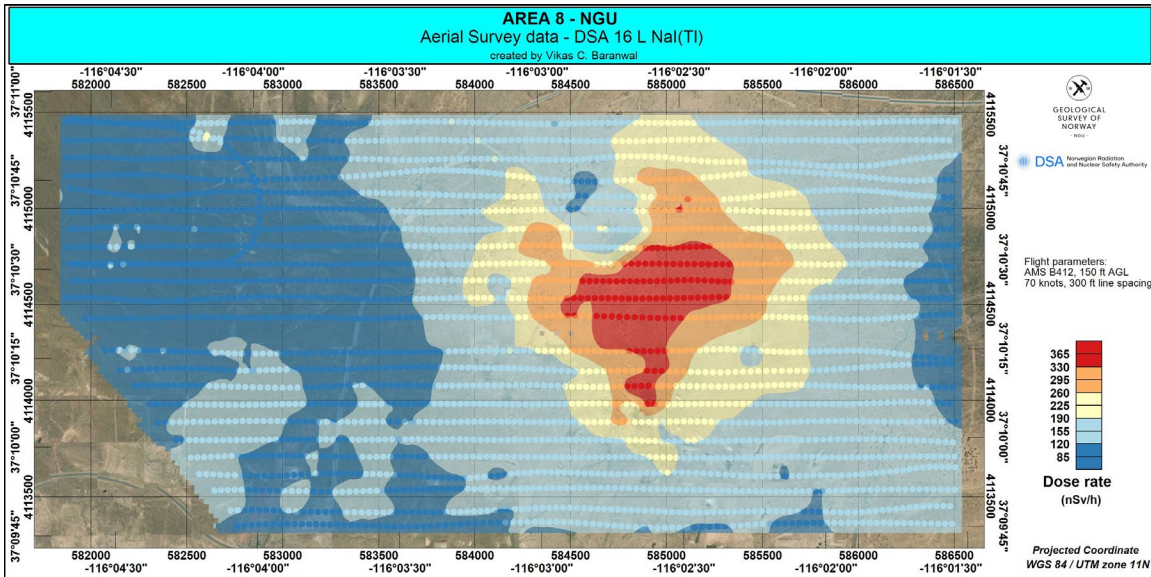


FIGURE 34. DOSE RATE FROM NNSS AREA 8 FROM DSA DATA.

NNSS AREA 11

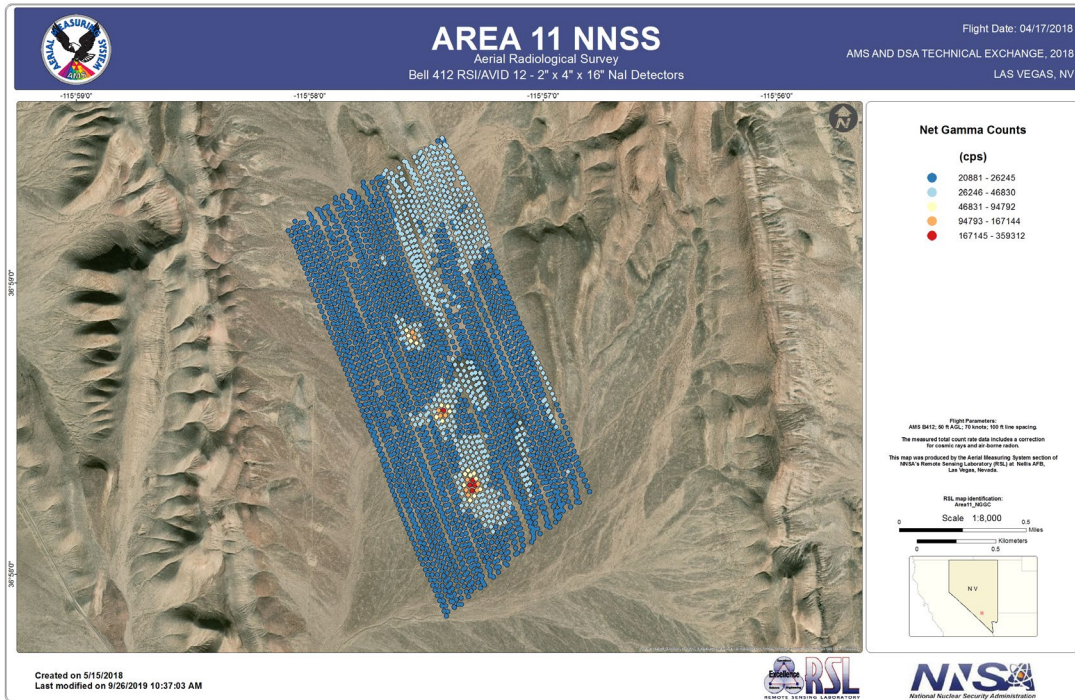


FIGURE 35. GROSS COUNTS FROM NNSS AREA 11 FROM AMS DATA.

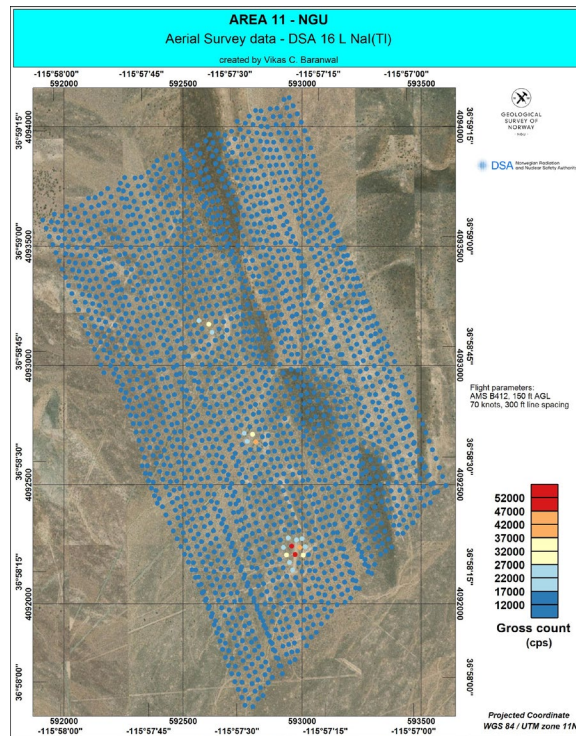


FIGURE 36. GROSS COUNTS FROM NNSS AREA 11 FROM DSA DATA.

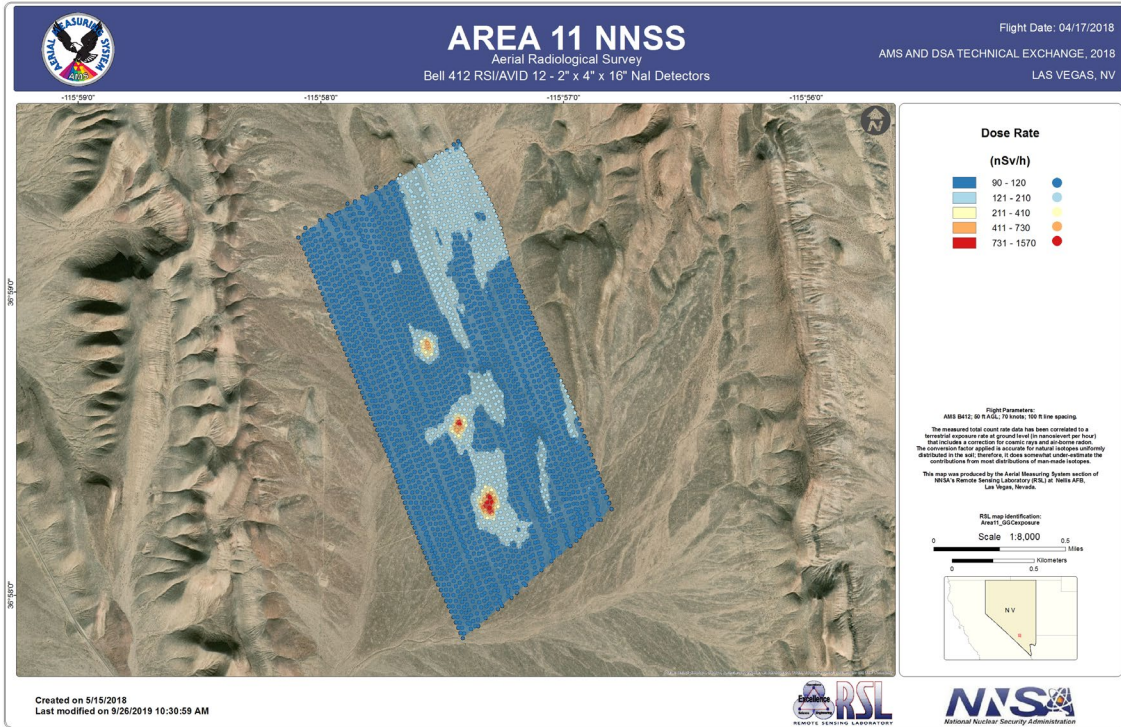


FIGURE 37. DOSE RATE FROM NNSS AREA 11.

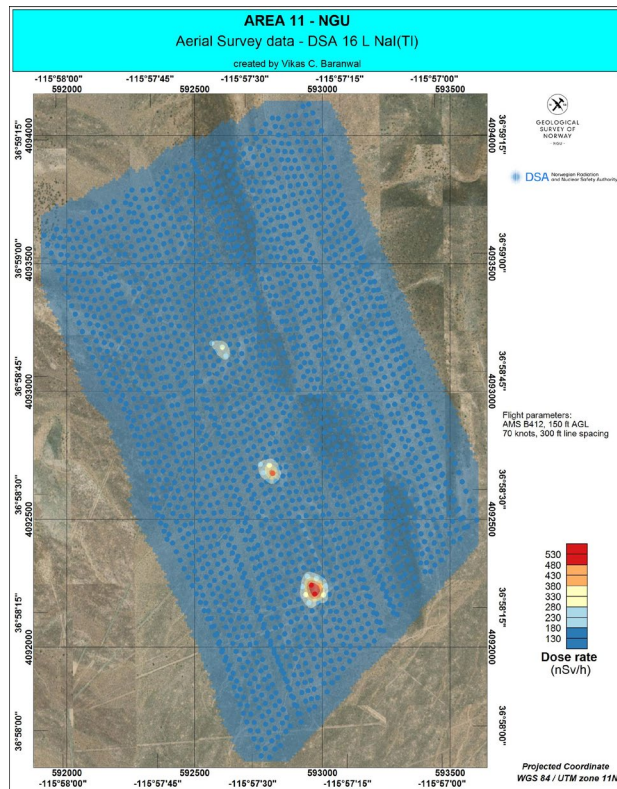


FIGURE 38. DOSE RATE FROM NNSS AREA 11 FROM DSA DATA.

NNSS AREA 30

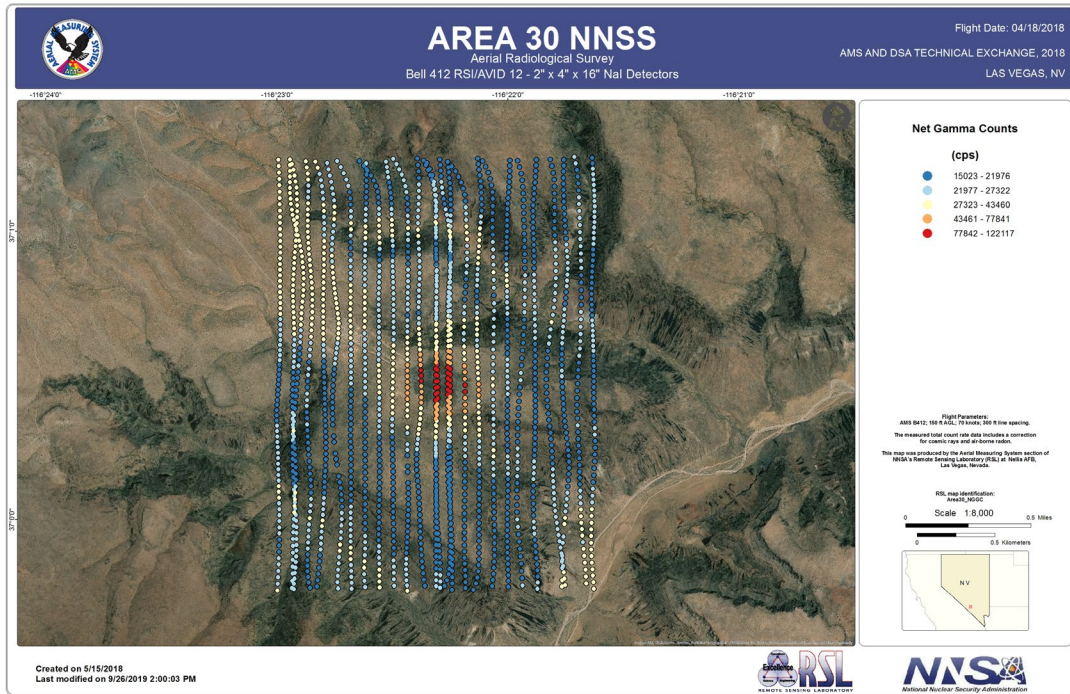


FIGURE 39. GROSS COUNTS FROM NNSS AREA 30 FROM AMS DATA.

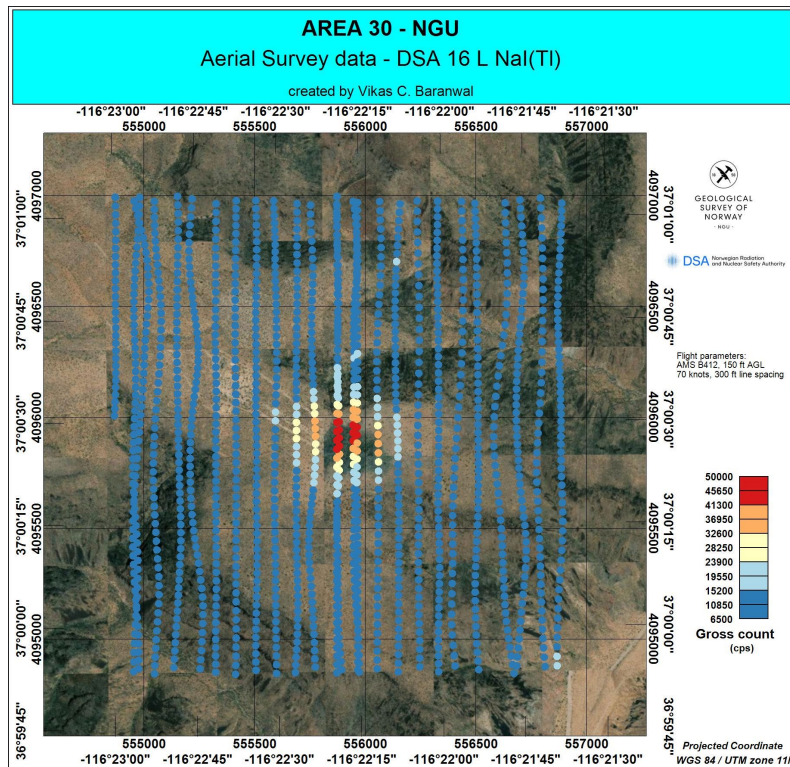


FIGURE 40. GROSS COUNTS FROM NNSS AREA 30 FROM DSA DATA.

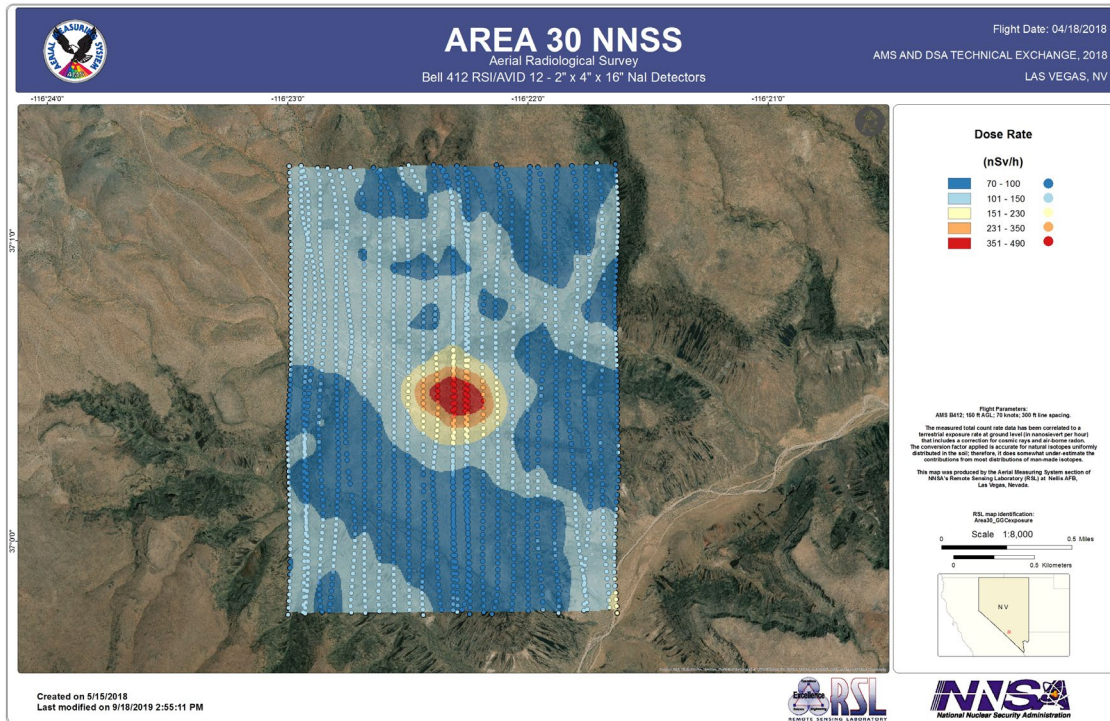


FIGURE 41. DOSE RATE FROM NNSS AREA 30 FROM AMS DATA.

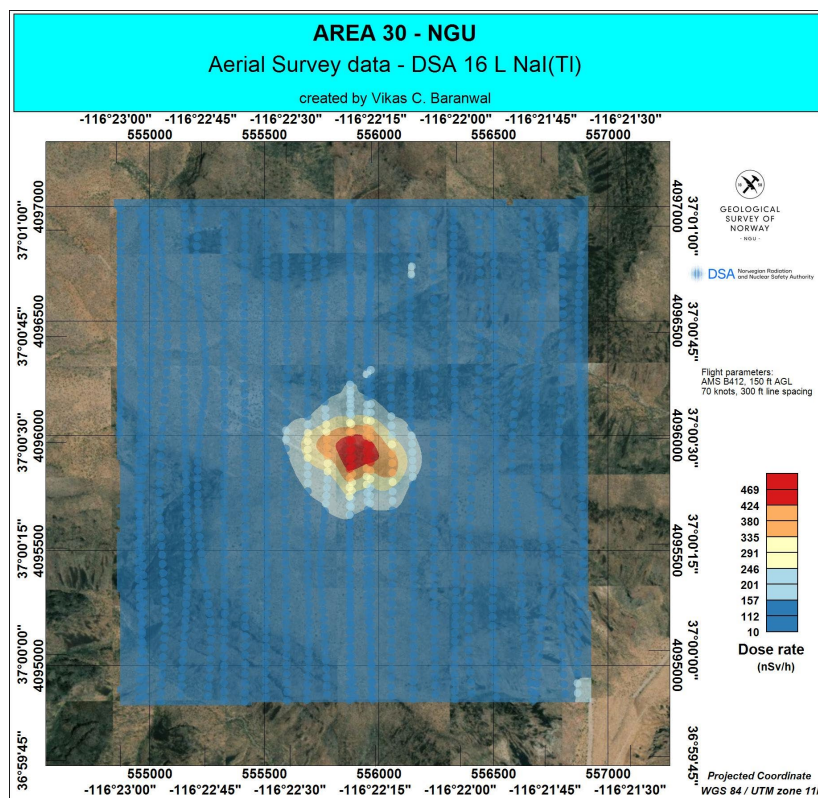


FIGURE 42. DOSE RATE FROM NNSS AREA 30 FROM DSA DATA.

CONCLUSION

The AMS-DSA technical exchange was an overall success. All the primary objectives of the aerial campaign were achieved. Both teams had the opportunity to become familiar with each other's capabilities and limitations. This exchange has strengthened both teams' confidence in our ability to jointly respond to a nuclear or radiological incident without significant questioning of each other's data quality or methods.

Differences in the measured and calculated net gross counts from AMS and DSA spectrometers could be attributed to the different crystal volumes, energy windows, and shielding. However, the dose rate parameters were calibrated from the same area (Lake Mohave) for both, which resulted in similar dose rate ranges for all areas surveyed.

A different approach for processing, gridding, and color scale for identifying individual nuclides are used by AMS and NGU for AMS and DSA spectrometer data respectively. Therefore, the distribution patterns for nuclides are not the same and vary a bit (shown in appendix B as extra extractions). NGU was able to detect K, U, Th, Am-241, Cs-137, and Eu-152 at various locations. However, at a select few locations, NGU was not able to detect some nuclides from DSA data (Table 8) so well as AMS detected from AMS data (e.g., Co-60 in area 8 and Eu-152 in Area 30).

A detailed investigation of the AMS and DSA spectrometer data is needed to identify the discrepancy between AMS and NGU results for individual nuclides. However, this discrepancy could be the result of a difference in the collected data (due to shielding), or different analysis methods used by the two organizations.

BIBLIOGRAPHY

- Briggs, I. (1974, February). Machine Contouring Using Minimum Curvature. *Geophysics*, 39(1), pp. 39-48.
- Bristow, Q. (1978). Application of Airborne Gamma-Ray Spectrometry in the Search for Radioactive Debris from the Russian Satellite Cosmos 954 (Operation "Morning Light"). *Current Research Part B Geological Survey of Canada Paper*, 78-1B, p. 151.
- Hendricks, T. J., & Riedhauser, S. R. (1999). *AN AERIAL RADIOLOGICAL SURVEY OF THE NEVADA TEST SITE*. Las Vegas: Bechtel Nevada Report DOE/NV/11718--324.
- Kogan, R. e. (1971). *Gamma Spectrometry of the Natural Environments and Formations*. Jerusalem: Israel Program for Scientific Translations.
- Oberlercher, G., & Seiberl, G. (1997). *Quantitative Cs-137 Distributions from Airborne Gamma Ray Data*. Vienna: International Atomic Energy Agency.
- Thørring, H., Baranwal, V., Ytre-Eide, M., Rønning, J., Mauring, A., Stampolidis, A., . . . Skuterud, L. (2019). Airborne Radiometric Survey of a Chernobyl-contaminated Mountain Area in Norway- Using Ground-level Measurements for validation. *Journal of Environmental Radioactivity*, 208-209(106004), 1-11.
- U.S. DOE Nevada Operations Office. (1978). *Operation Morning Light, A Non-Technical Summary of U.S. Participation*. Las Vegas: U.S. DOE Report NV-198.

APPENDIX A: PERSONNEL

TABLE A1. DOE PERSONNEL.

Name	Position
Piotr Wasiolek	AMS Task Lead
Rusty Malchow	AMS Scientist
Daniel Haber	AMS Scientist
Leslie Winfield	Federal AMS Manager
Kirk Czap	NNSA NA-81
Michael Toland	Pilot
Sue Roberts	Pilot
Ed Zachman	Helicopter Mechanic
Jezabel Stampahar	AMS Data Analyst
Tom Stampahar	AMS Equipment Specialist

TABLE A2. DSA/NGU PERSONNEL.

Name	Position
Morten Sickel	DSA Task Lead ¹
Tanya H Hevroey	DSA Scientist ²
Martin Album Ytre-Eide	DSA Scientist/Data analyst ³
Vikas Baranwal	NGU Scientist

1. Now at NORSAR, Norway
2. Now at Norwegian Institute for Air Research (NILU)
3. Now at Norwegian Environment Agency

APPENDIX B: ADDITIONAL EXTRACTIONS

In this section, we present additional extraction of three natural radio-elements K, U, Th and four anthropogenic radio-nuclides Cs-137, Co-60, Eu-152 and Am-241 from areas 3, 8, 11 and 30 by AMS and NGU. Both have used different way of extraction as described in the section Data Evaluation Methods. NGU could not plot concentration of K, U and Th because DSA spectrometer was not calibrated to calculate stripping ratios and sensitivity coefficients etc. to facilitate the calculation of the concentration of these radioelements therefore, NGU has plotted their corresponding window counts in counts/second (cps).

TABLE B1. MAXIMUM COUNTS/SECOND/CHANNEL FOR VARIOUS RADIO-ELEMENTS FROM VARIOUS NNSS TEST AREAS.

Element Area	Cs-137	Co-60	Eu-152	Am-241
Area 3	52	1	11	75
Area 8	42	1	2	718
Area 11	2	1	3	3154
Area 30	33	2	6	132

Table B1 shows maximum number of counts/second/channel calculated from the various areas according to TABLE 6 and Equation 8 by NGU. Table B1 shows very low count rate/channel for Co-60 for all the areas which means Co-60 was not found in any of these areas from DSA data. Similarly, Cs-137 was not found in areas 11 and Eu-152 was not found in areas 8, 11 and 30, respectively in DSA data. Am-241 was found in all the areas in DSA data and it was most and least abundant in areas 11 and 3, respectively.

Table B2 summarizes list of anthropogenic nuclides found from AMS data using AMS extraction method and from DSA data using NGU extraction method. AMS's Gaussian extraction method from AMS data has shown the presence of Co-60 in area 8 and Eu-152 in area 30. It also confirmed that only Am-241 was present in area 11.

Table B2. ANTHROPOGENIC RADIO-NUCLIDES FOUND FROM AMS DATA BY AMS EXTRACTION METHOD AND FROM DSA DATA BY NGU EXTRACTION METHOD FROM VARIOUS NNSS TEST AREAS.

Isotope \ Area	Cs-137		Co-60		Eu-152		Am-241	
	AMS	NGU	AMS	NGU	AMS	NGU	AMS	NGU
Area 3	Y	Y	N	N	Y	Y	Y	Y
Area 8	Y	Y	Y	N	N	N	Y	Y
Area 11	N	N	N	N	N	N	Y	Y
Area 30	Y	Y	N	N	Y	N	Y	Y

GOVERNMENT WASH

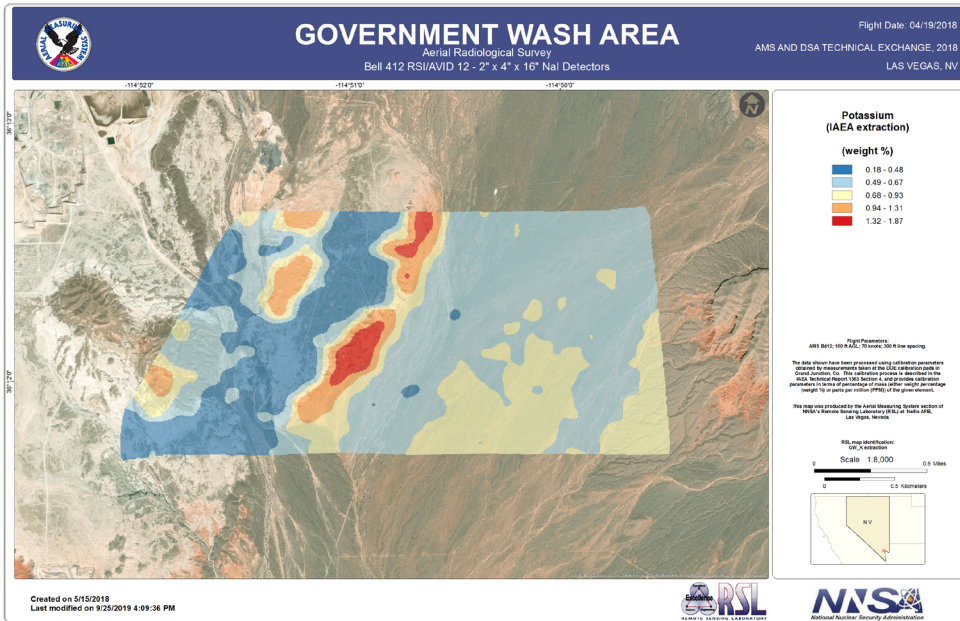


FIGURE 43. POTASSIUM (%) FROM THE NATURAL BACKGROUND AREA (GOVERNMENT WASH) FROM AMS DATA.

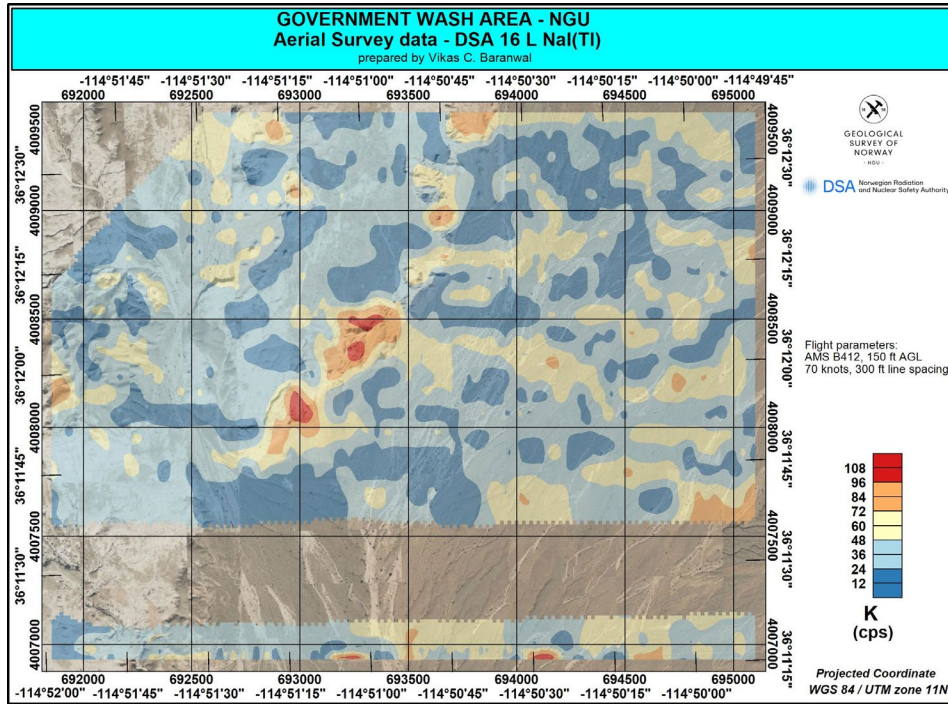


FIGURE 44. POTASSIUM (CPS) FROM THE NATURAL BACKGROUND AREA (GOVERNMENT WASH) FROM DSA DATA.

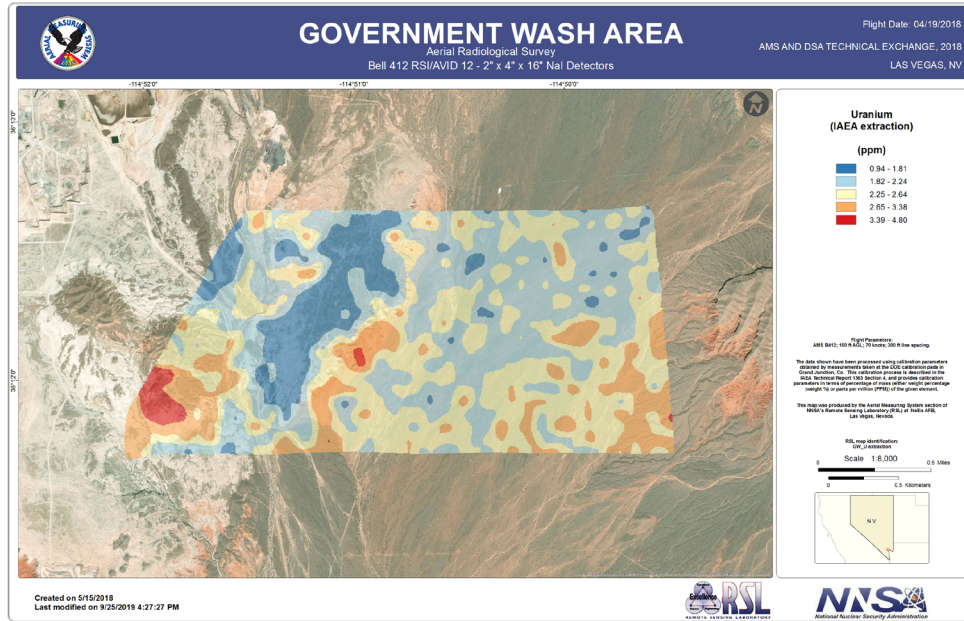


FIGURE 45. URANIUM (PPM) FROM THE NATURAL BACKGROUND AREA (GOVERNMENT WASH) FROM AMS DATA.

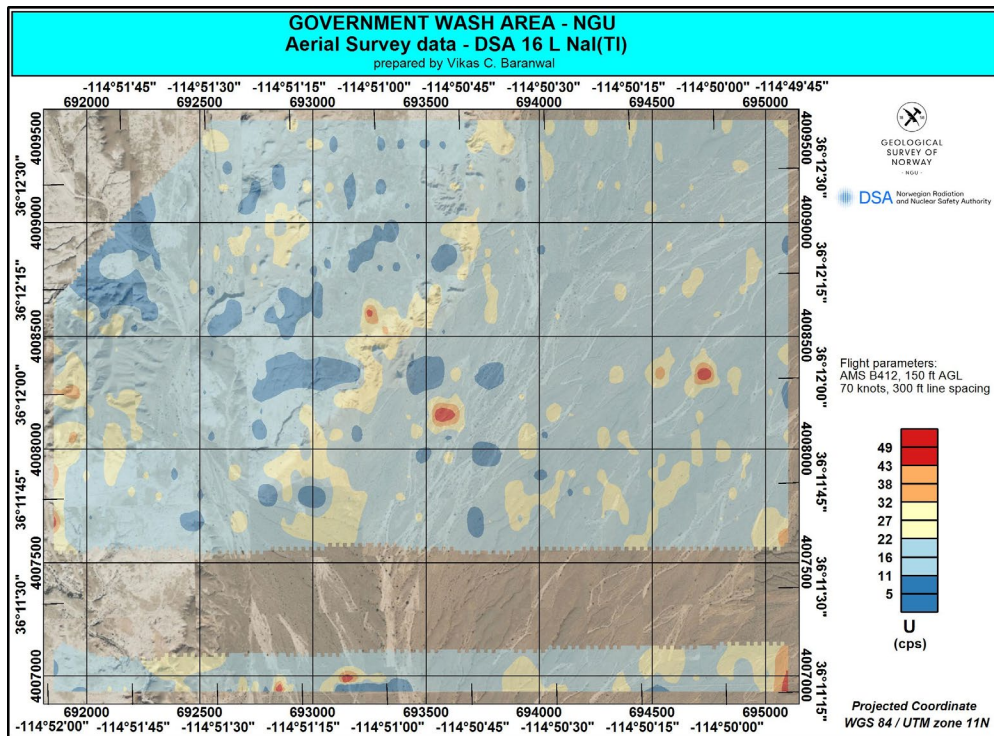


FIGURE 46. URANIUM (CPS) FROM THE NATURAL BACKGROUND AREA (GOVERNMENT WASH) FROM DSA DATA.

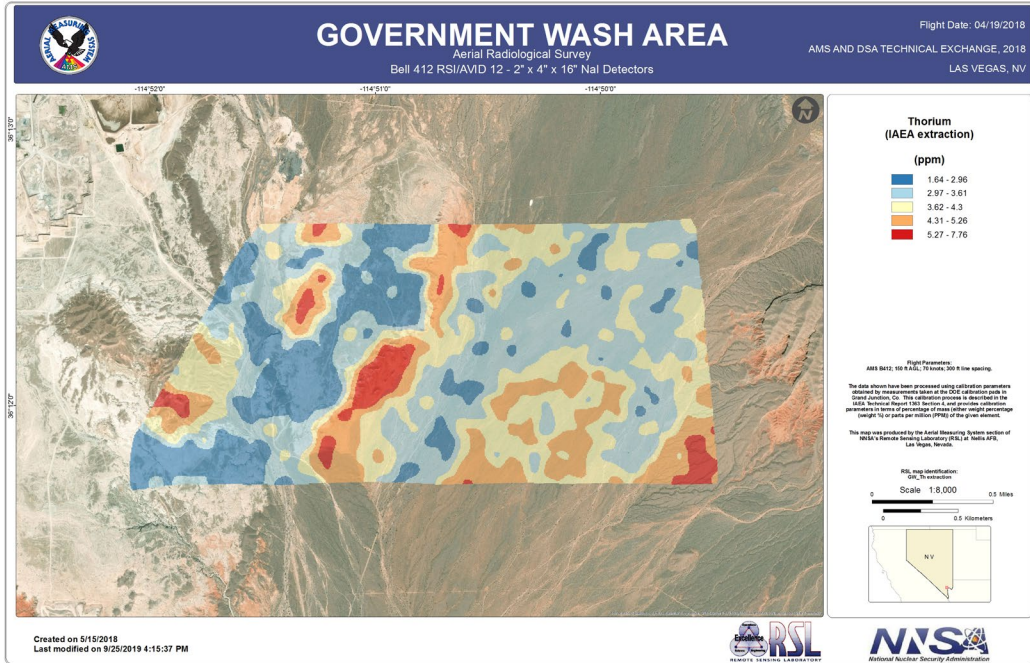


FIGURE 47. THORIUM (PPM) FROM THE NATURAL BACKGROUND AREA (GOVERNMENT WASH) FROM AMS DATA.

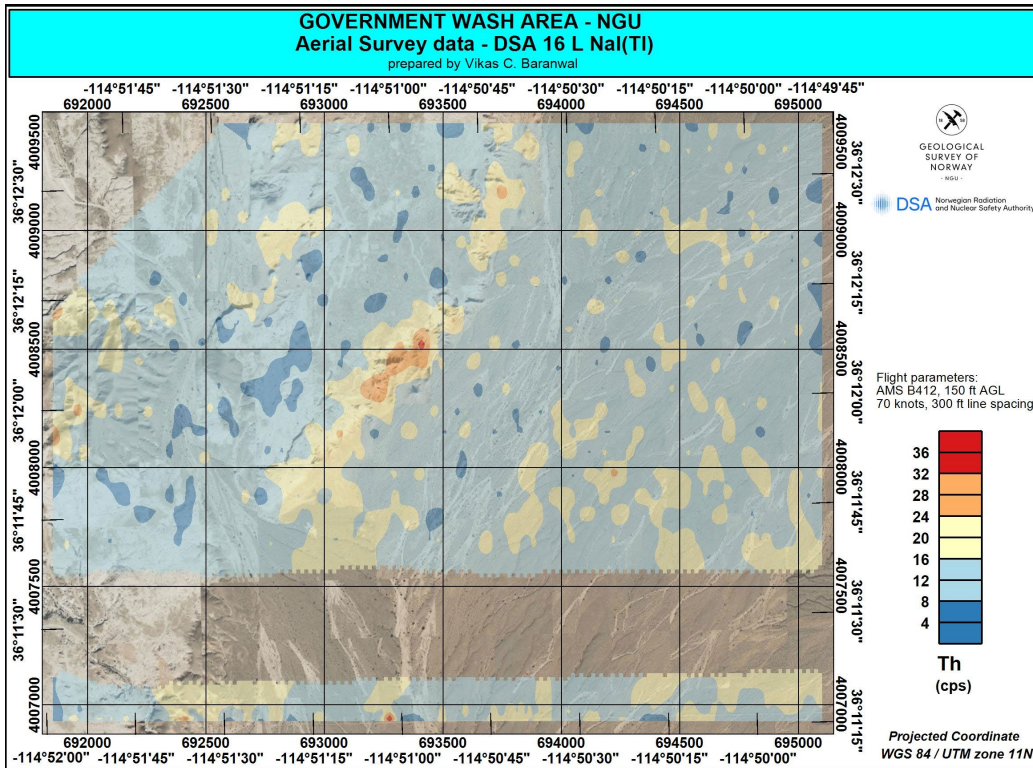


FIGURE 48. THORIUM (CPS) FROM THE NATURAL BACKGROUND AREA (GOVERNMENT WASH) FROM DSA DATA.

AREA 3

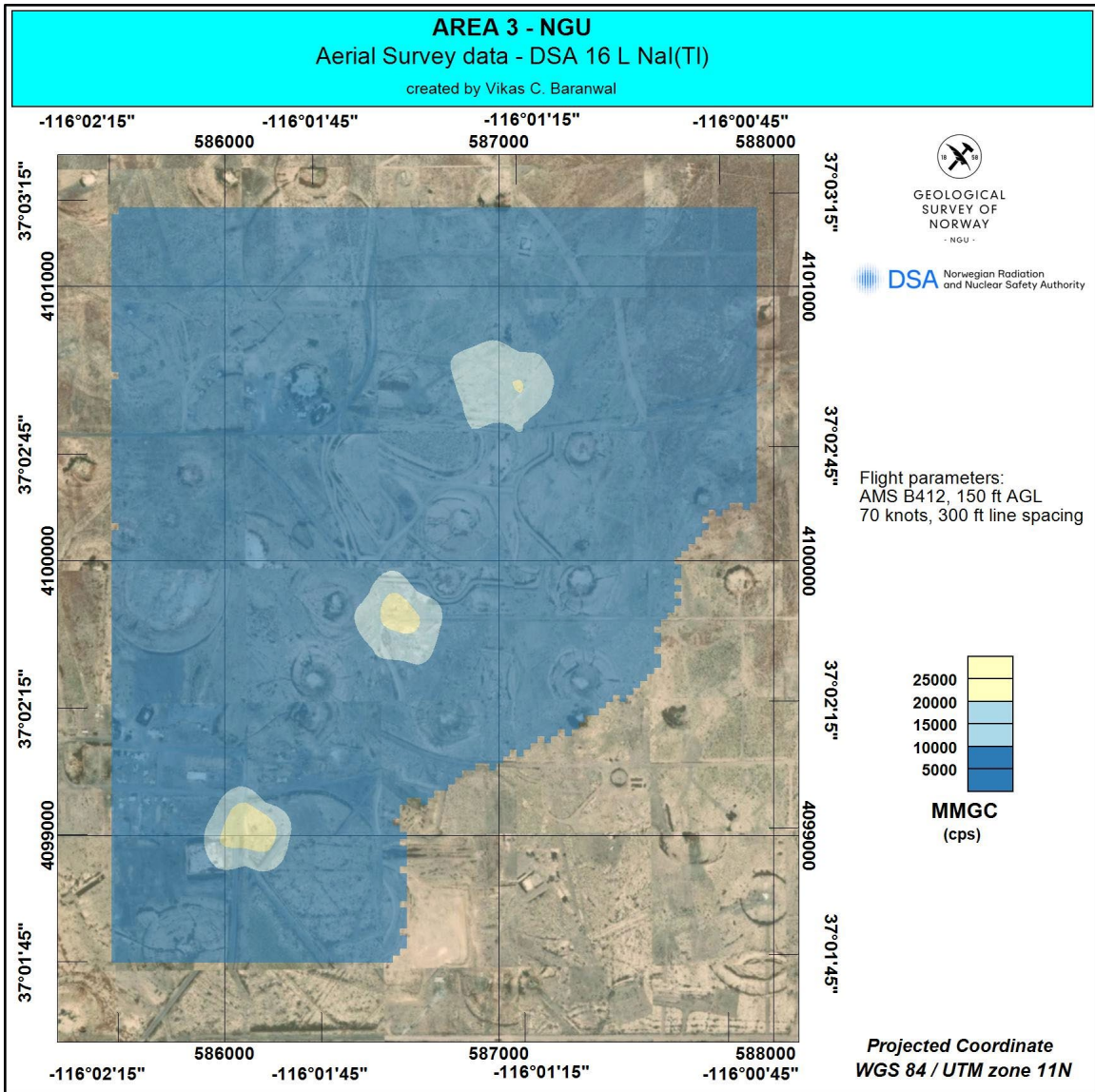


FIGURE 49. MMGC (C_{MM}) FROM NNSS AREA 3 FROM DSA DATA

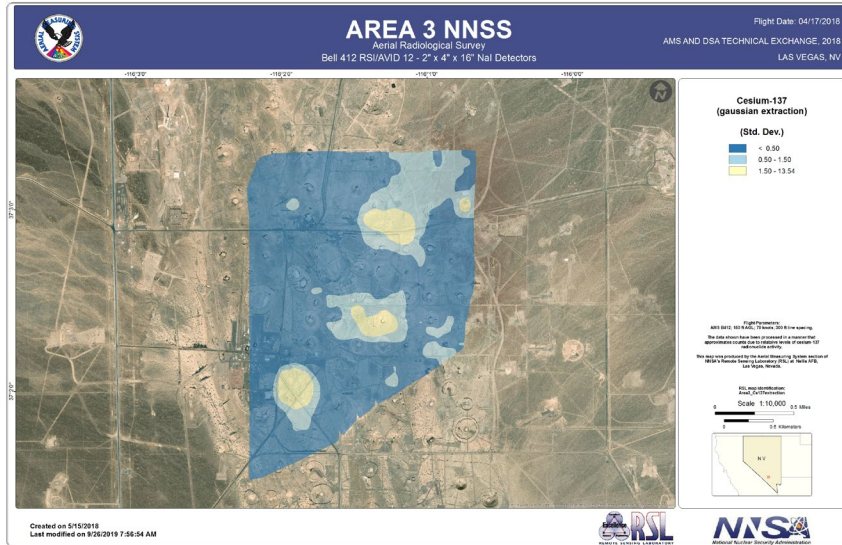


FIGURE 50. CS-137 EXTRACTION (GAUSSIAN) FROM NNSS AREA 3 FROM AMS DATA.

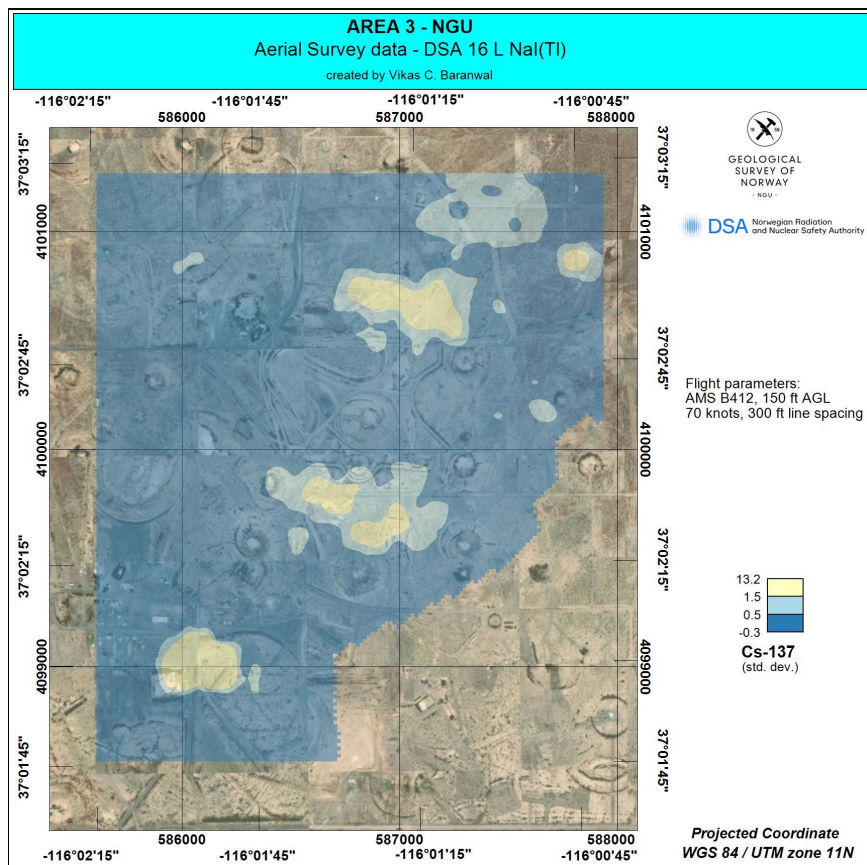


FIGURE 51. CS-137 EXTRACTION (SPECTRAL WINDOW) FROM NNSS AREA 3 FROM DSA DATA.

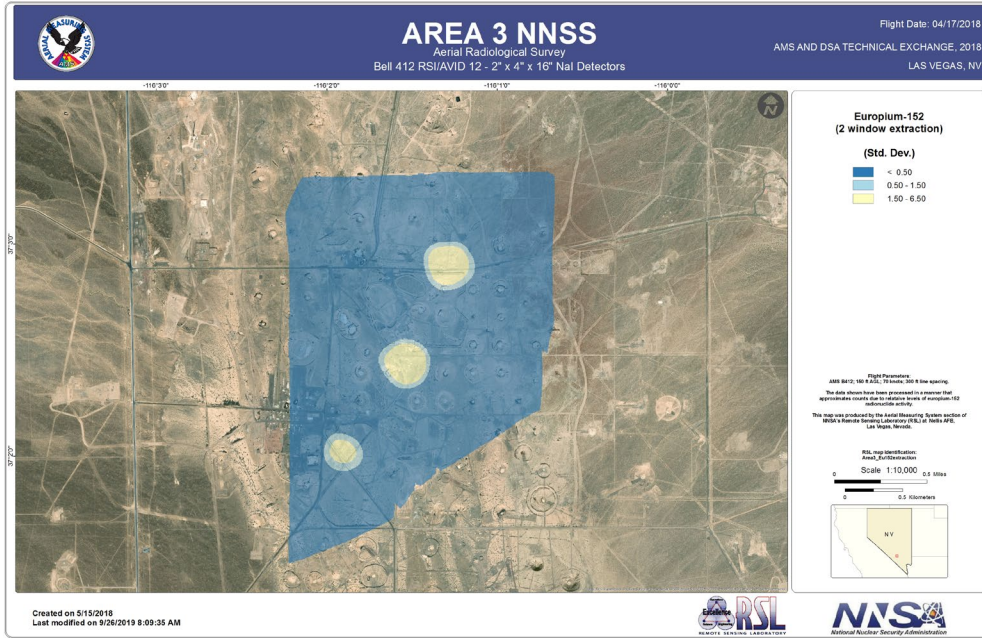


FIGURE 52. EU-152 EXTRACTION (TWO-WINDOW) FROM NNSS AREA 3 FROM AMS DATA.

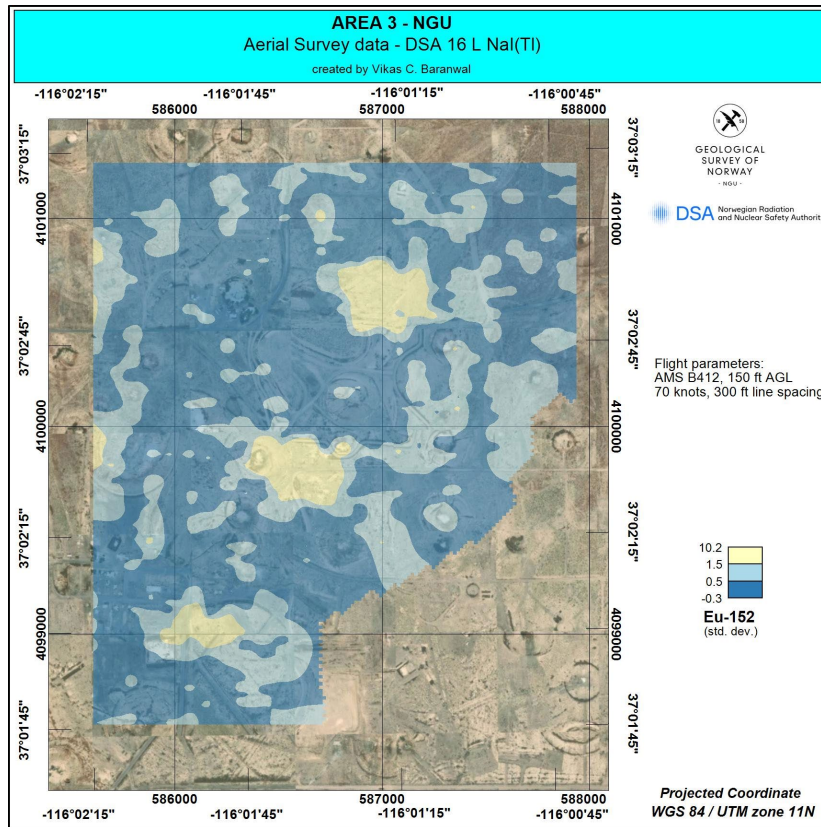


FIGURE 53. EU-152 EXTRACTION (SPECTRAL WINDOW) FROM NNSS AREA 3 FROM DSA DATA.

AREA 8

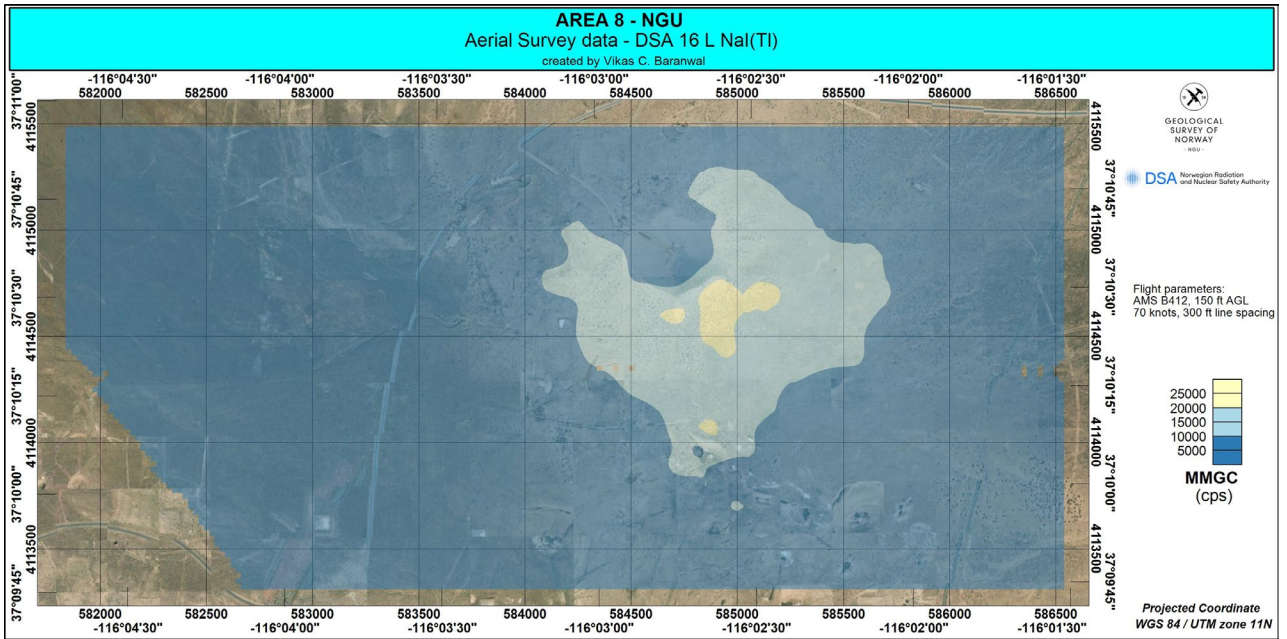


FIGURE 56. MMGC (C_{MM}) FROM NNSS AREA 8 FROM DSA DATA.

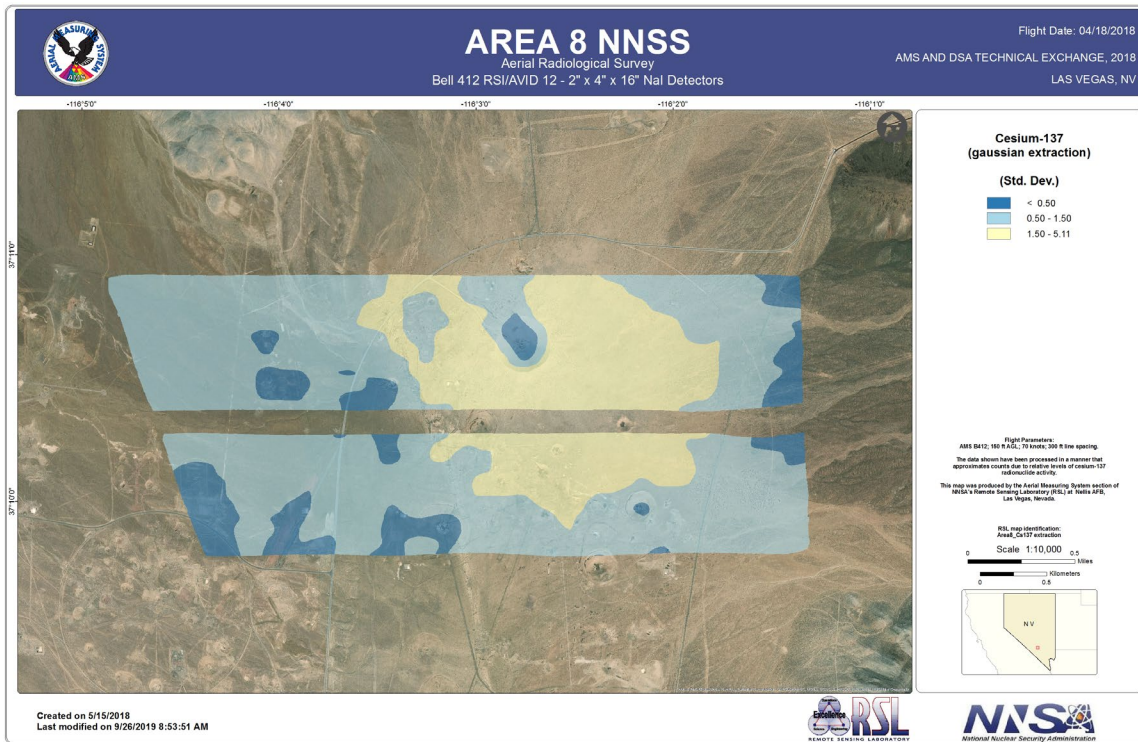


FIGURE 57. CS-137 EXTRACTION (TWO-WINDOW) FROM NNSS AREA 8 FROM AMS DATA.

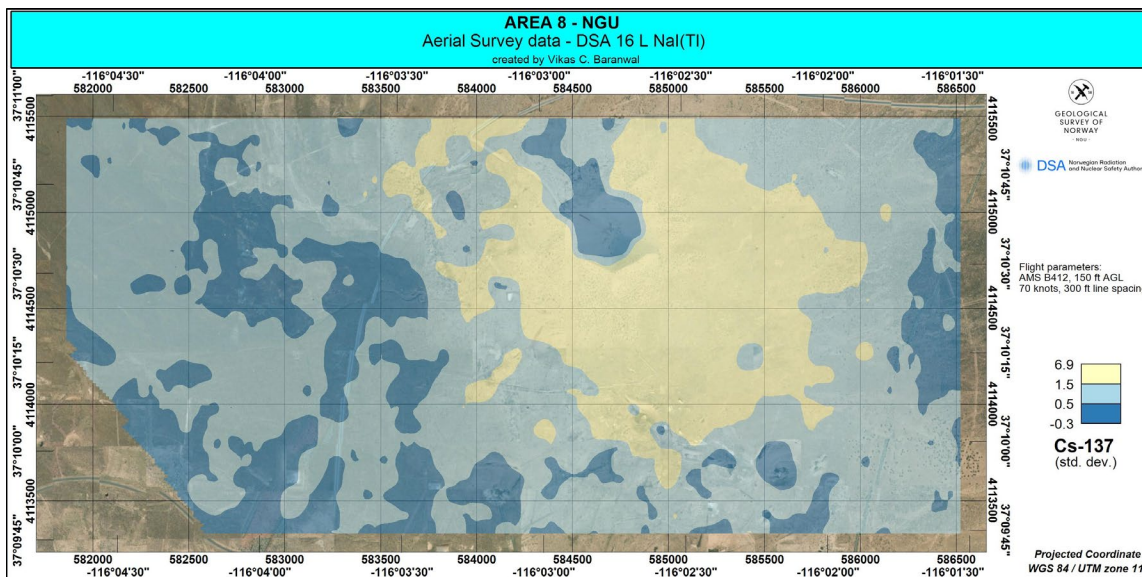


FIGURE 58. CS-137 EXTRACTION (SPECTRAL WINDOW) FROM NNSS AREA 8 FROM DSA DATA.

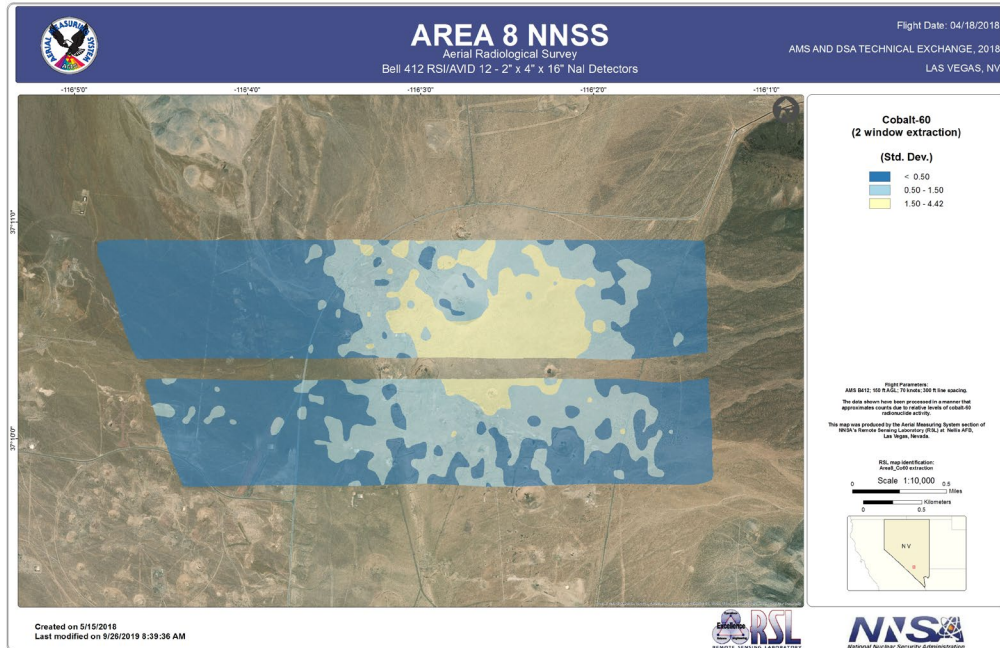


FIGURE 59. CO-60 EXTRACTION (TWO-WINDOW) FROM NNSA AREA 8 FROM AMS DATA.

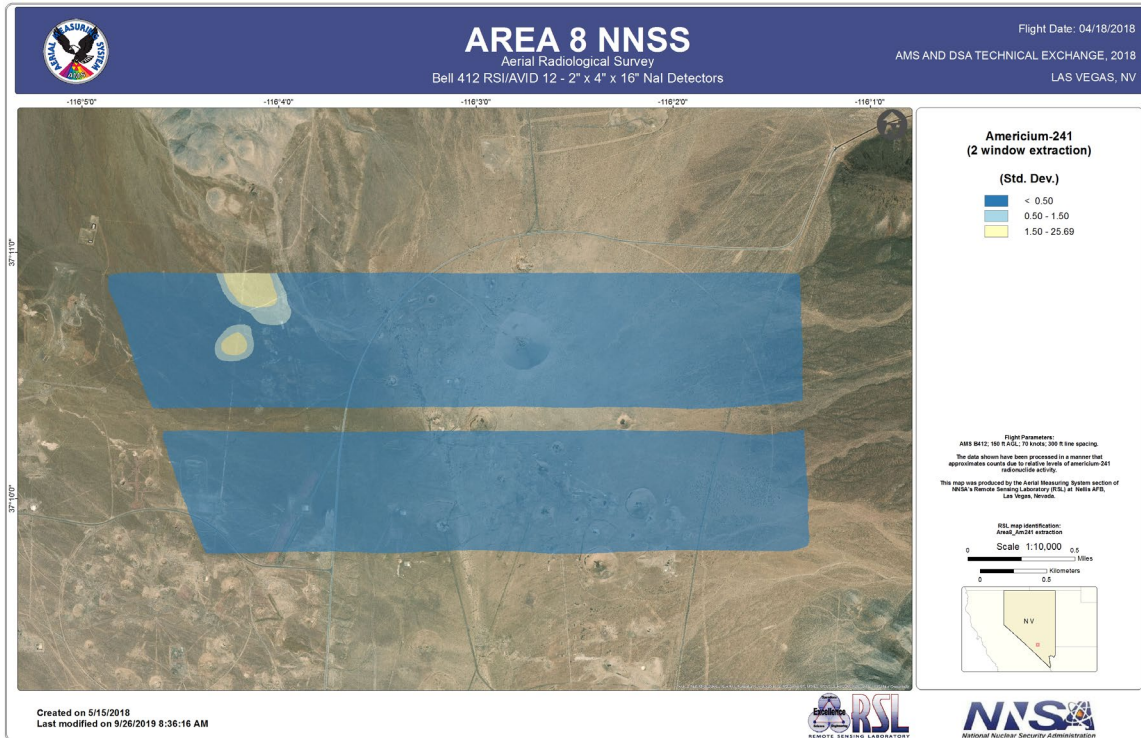


FIGURE 60. AM-241 EXTRACTION (TWO-WINDOW) FROM NNSS AREA 8 FROM AMS DATA.

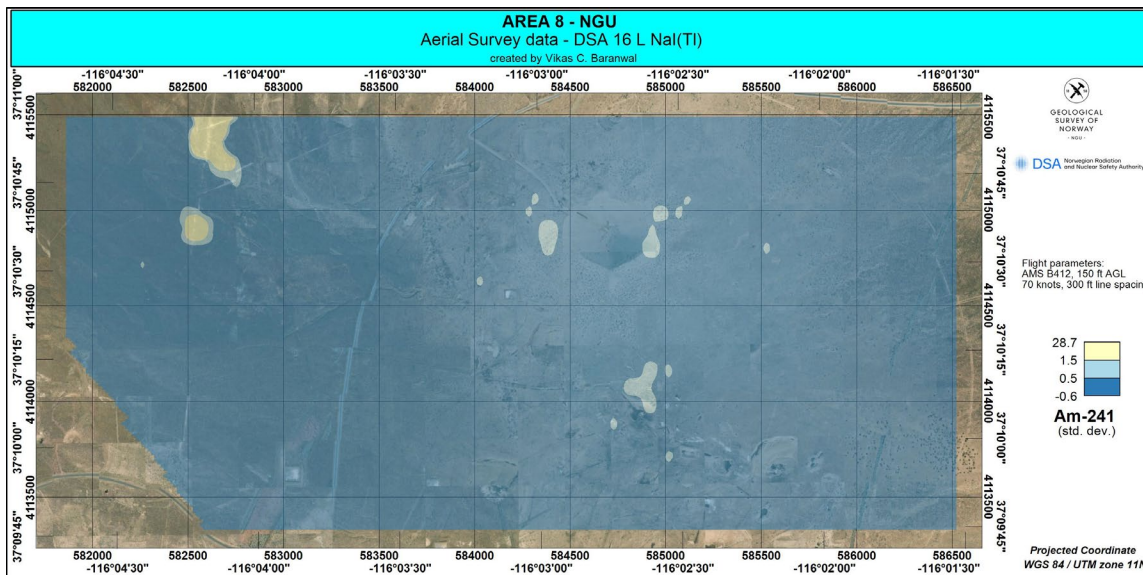


FIGURE 61. AM-241 EXTRACTION (SPECTRAL WINDOW) FROM NNSS AREA 8 FROM DSA DATA.

AREA 11

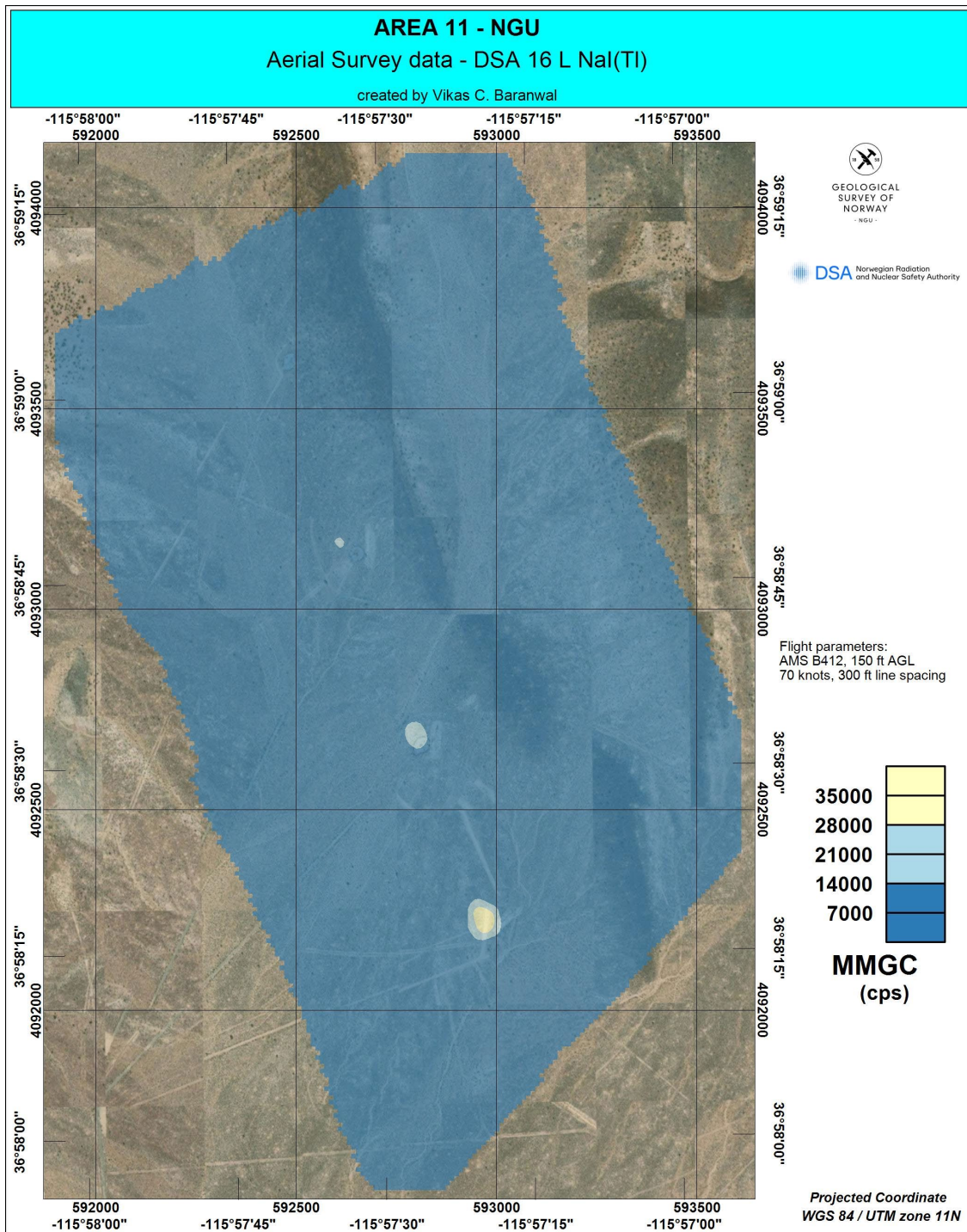


FIGURE 62. MMGC (C_{MM}) FROM NNSS AREA 11 FROM DSA DATA.

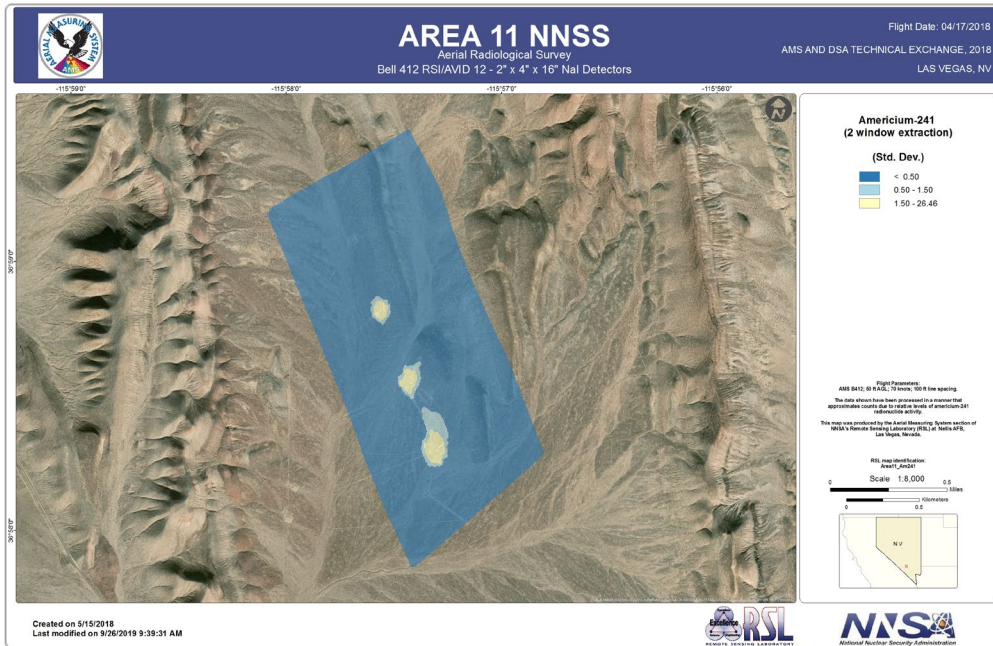


FIGURE 63. AM-241 EXTRACTION (TWO-WINDOW) FROM NNSS AREA 11 FROM AMS DATA.

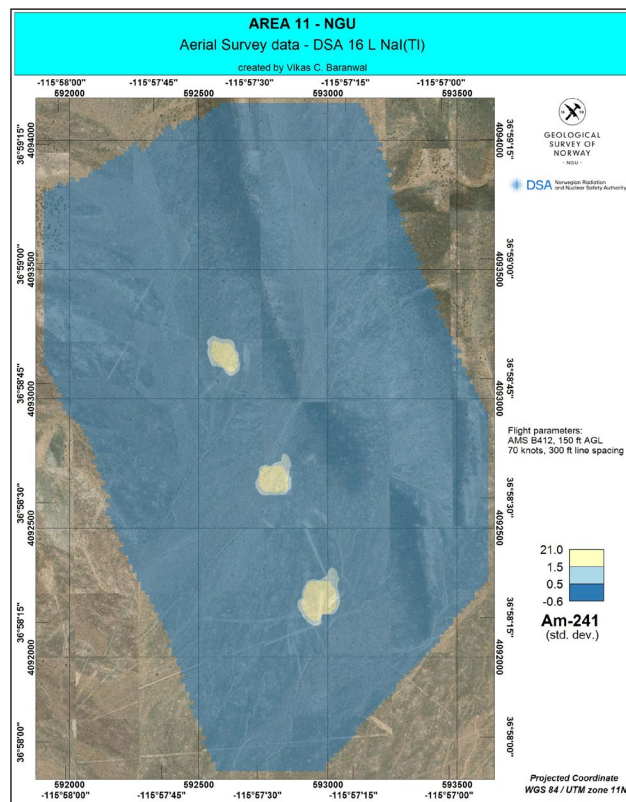


FIGURE 64. AM-241 EXTRACTION (SPECTRAL WINDOW) FROM NNSS AREA 11 FROM DSA DATA.

AREA 30

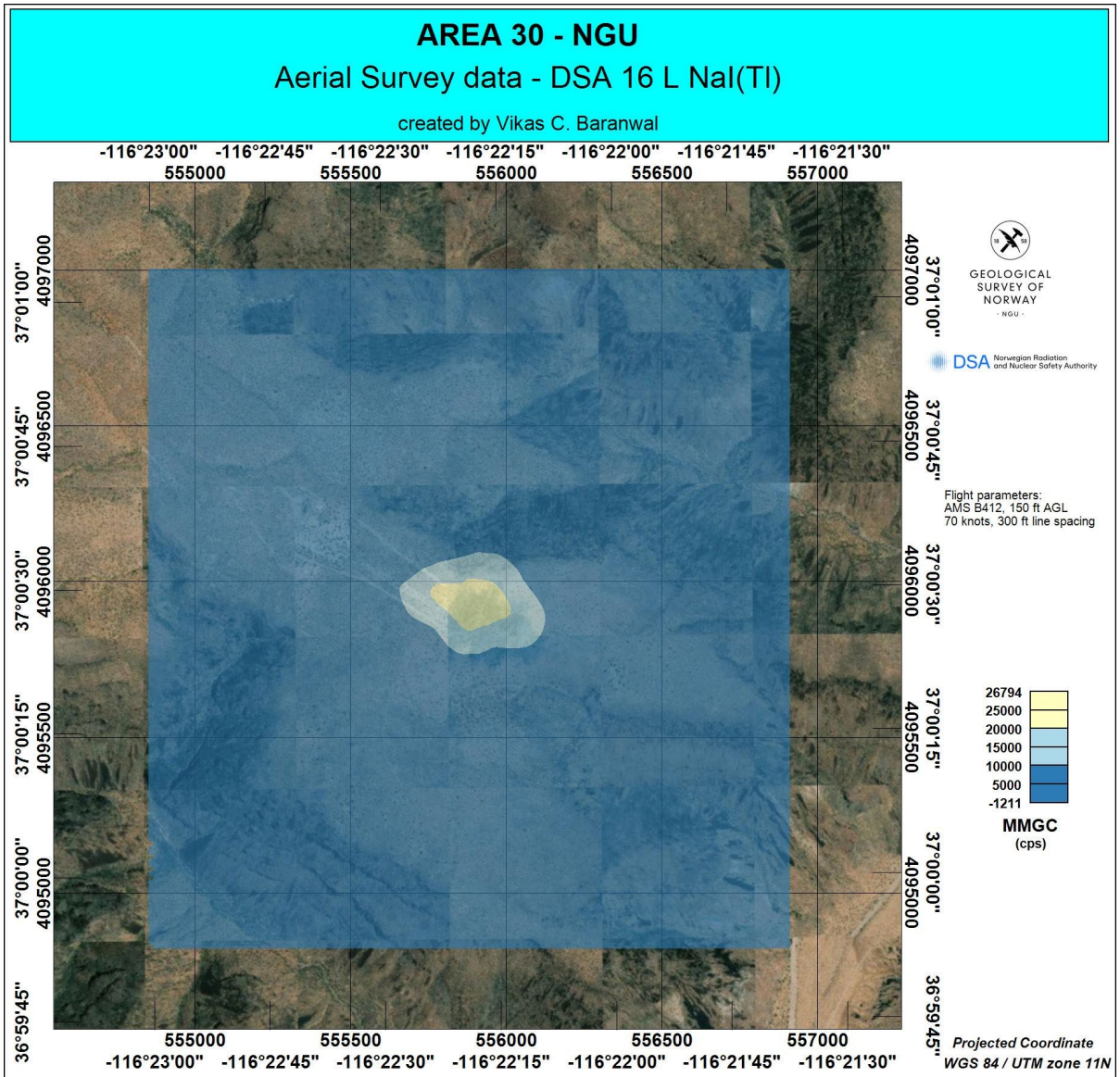


FIGURE 65. MMGC (C_{MM}) FROM NNSS AREA 30 FROM DSA DATA.

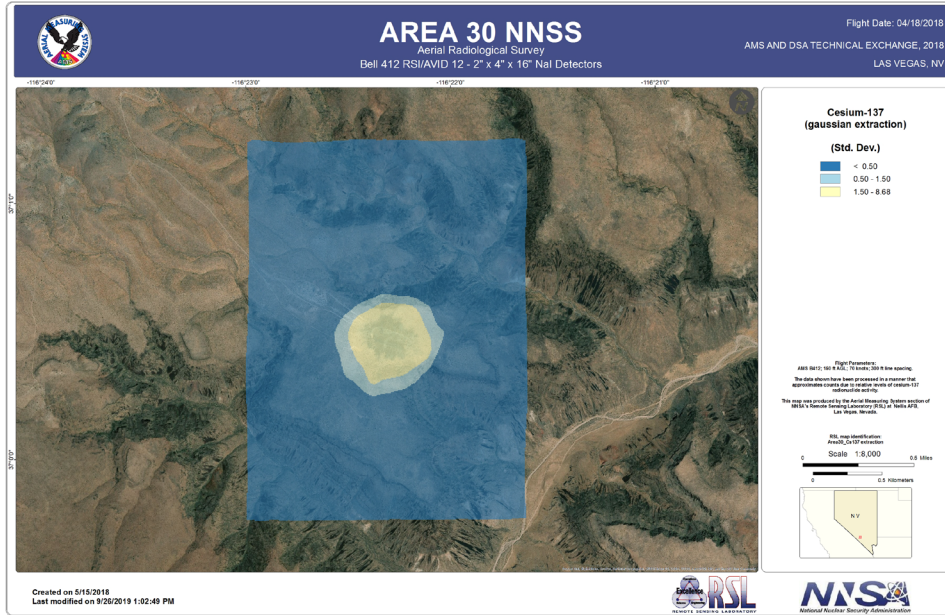


FIGURE 66. CS-137 EXTRACTION (TWO-WINDOW) FROM NNSS AREA 30 FROM AMS DATA.

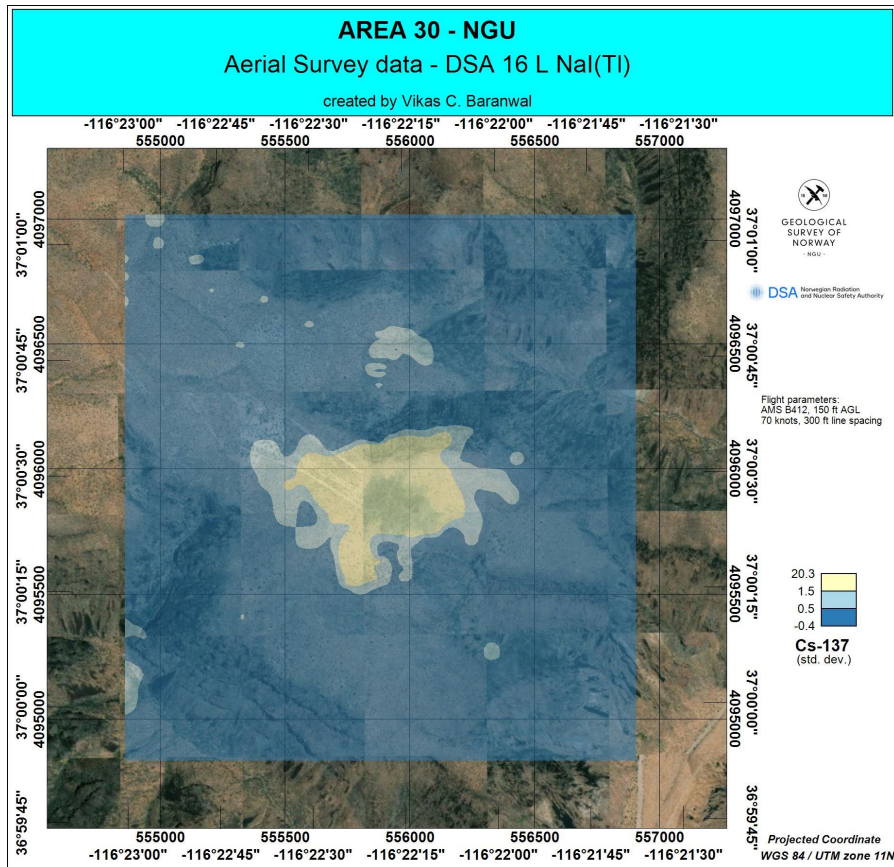


FIGURE 67. Cs-137 EXTRACTION (SPECTRAL WINDOW) FROM NNSS AREA 30 FROM DSA DATA.

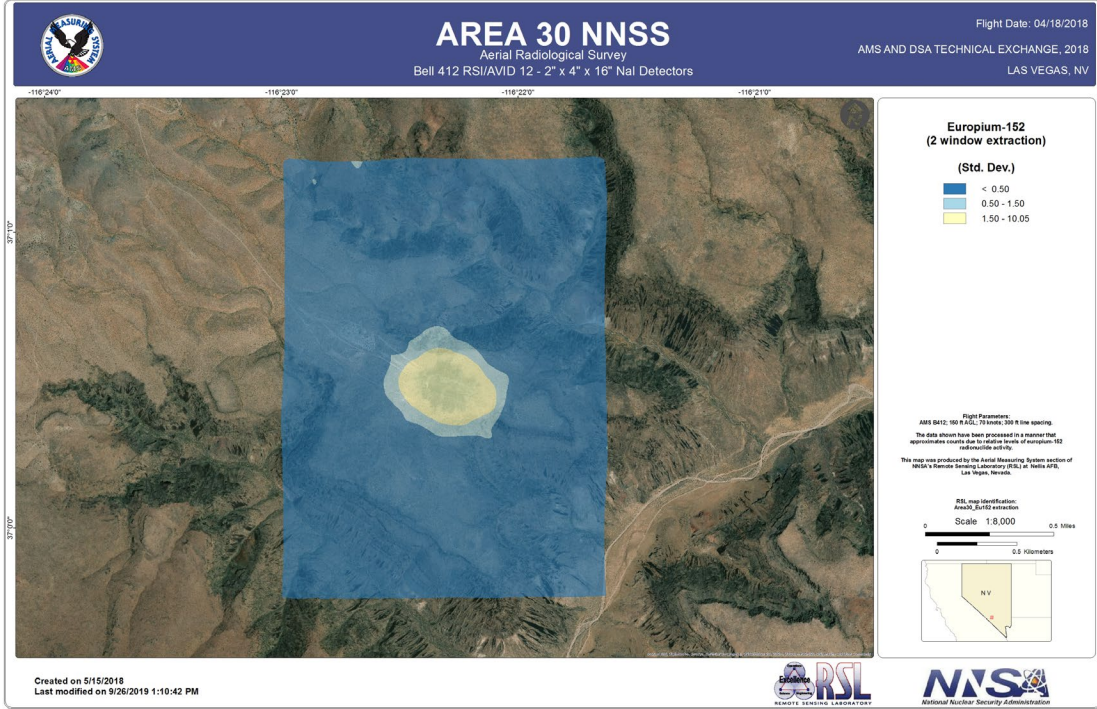


FIGURE 68. EU-152 EXTRACTION (TWO-WINDOW) FROM NNSS AREA 30 FROM AMS DATA.

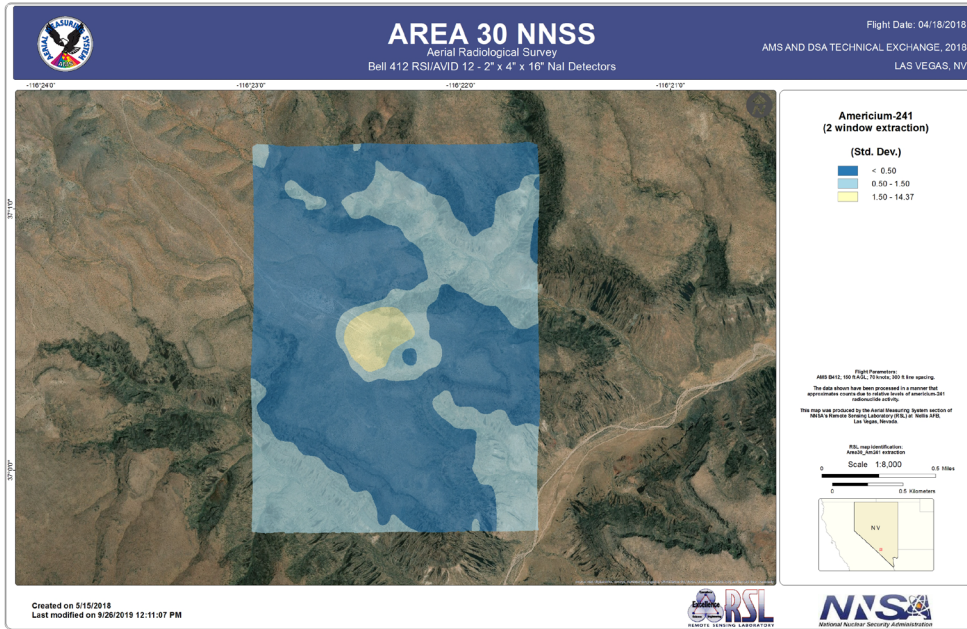


FIGURE 69. AM-241 EXTRACTION (TWO-WINDOW) FROM NNSS AREA 30 FROM AMS DATA.

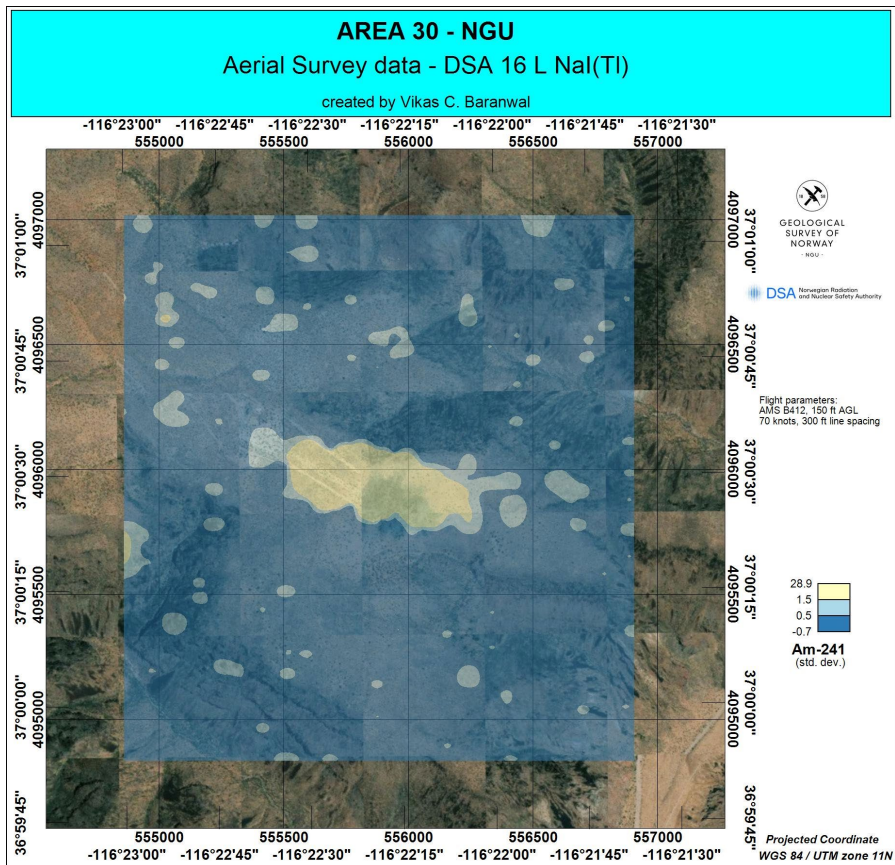


FIGURE 70. AM-241 EXTRACTION (SPECTRAL WINDOW) FROM NNSS AREA 30 FROM DSA DATA.